2.3 Department of Heterogeneous Catalysis

Director:

Ferdi Schüth (born 1960)

Further group leaders:

Frank Marlow (born 1960)

Roberto Rinaldi (born 1979)

Wolfgang Schmidt (born 1962)

Harun Tüysüz (born 1978)
group leader since 2012

Claudia Weidenthaler (born in 1965)
group leader since 2012

Curriculum Vitae: Ferdi Schüth

1960	Born in Allagen (now Warstein), Germany
1978-84	Chemistry studies at the Westfälische Wilhelms-Universität Münster, Diploma October 1984
1983-88	Law Studies at the Westfälische Wilhelms-Universität Münster, First State Examination February 1989
1984-88	Doctoral studies in the group of E. Wicke, Institute of Physical Chemistry, Münster, Dr. rer. nat. June 1988
1988-89	Post-doc at the Department of Chemical Engineering and Materials Science, University of Minnesota, USA, L. D. Schmidt
1989-95	Wissenschaftlicher Assistent (Assistant Professor) at the Institute of Inorganic and Analytical Chemistry of the Universität Mainz, K. Unger, Habilitation February 1995
1993	Visiting Assistant Professor at the Department of Chemistry, University of California at Santa Barbara, USA, G. D. Stucky
1995-98	Full Professor of Inorganic Chemistry at the Johann-Wolfgang-Goethe Universtität Frankfurt
1998-	Scientific Member of the Max Planck Society and Director at the Max-Planck-Institut für Kohlenforschung, Mülheim/Ruhr

Awards and Honors

1989	Award for outstanding Ph.D. thesis
1991	Boehringer-Ingelheim Research Award
2001	Award des Stifterverbandes für die Deutsche Wissenschaft
2003	Gottfried Wilhelm Leibniz Award of the Deutsche Forschungsgemeinschaft
2007	Honorary Professor of Dalian University of Technology, China
2008	Elected member of German Academy of Science Leopoldina
2009	Guest Professor Beijing University, China
2009	European Research Council Advanced Grant
2010	Heisenberg-Medaille of the Alexander von Humboldt Foundation
2010	Elected member of the Nordrhein-Westfälische Akademie der Wissenschaften und der Künste
2010	Nominated for the Deutscher Zukunftspreis 2010
2011	Ruhrpreis für Wissenschaft und Kunst (Ruhr Award for Science and Arts)

2011	Wöhler-Award for resource-saving processes
2011	Hamburger Wissenschaftspreis (Hamburg Award for Science)
2012	Wilhelm-Klemm-Preis of the GDCh
2013	Chemical-Engineering-Medal of the ETH Zürich

Other Activities / Committees

1995-1997	Managing Director of the Institute of Inorganic Chemistry, Frankfurt University
1995-2001	Coordinator of the DFG-Schwerpunktprogramm "Nanoporous Crystals"
1994	Member of the Dechema Arbeitsausschuss "Heterogene Katalyse"
1995-2005	Member of the Dechema Arbeitsausschuss "Zeolithe"
1996-2004	Member of the Dechema Arbeitsausschuss "Mikroreaktionstechnik"
1996-	Member of the Editorial Board, *Microporous Materials*
1998	Member of the Editorial Board, *Advanced Materials*
1998-2005	Chairman of the Dechema Arbeitsausschuss "Zeolithe"
1999-	Founder, Chairman of the Board and of the Scientific Advisory Board hte AG
1999-2005	Member of the Kuratorium, *Nachrichten aus der Chemie*
2000-	Member of the Dechema Board of Governors
2000-	Member of the Selection Committee for the Humboldt Award
2001-	Member of the IZA-Council
2001-	Chairman of the IZA Commission on Mesoporous Materials
2001-2006	Member of the Editorial Board, *Chemistry of Materials*
2002-	Member of the IMMA-Council
2002-2007	Member of the Selection Committee Heinz Maier-Leibniz Award
2003-2005	Managing Director of the Max-Planck-Institut für Kohlenforschung, Mülheim/Ruhr
2003-2007	Member of the Deutsche Forschungsgemeinschaft Senate Commission for SFB
2003-2010	Chairman of the Selection Committee, Alexander von Humboldt Award
2003-	Member of the Editorial Board "QSAR-Combinatorial Science"
2003-	Member of the International Expert Commission Elitenetzwerk Bayern
2004-2008	Member of the Kuratorium Universität Duisburg-Essen
2004-	Member of the Editorial Board, *Chemical Communications*
2004-	Member of the Scientific Commission of the State of Niedersachsen
2004-	Member of the GDCh Board of Governors

2004-	Chairman of the Dechema Forschungsausschuss “Chemical Reaction Engineering”
2005-	Chairman of the Investment Committee “Life Science, Materials and Energy” of the German High-Tech Fund
2005-	Member of the Editorial Advisory Board, *Chemical Engineering & Technology*
2005-	Member of the Expert Commission Elitenetzwerk Bayern
2006-	Editor, *Chemistry of Materials*
2006-	Member of the Advisory Board, *Chemistry–An Asian Journal*
2007-	Member of the Editorial Board, *Advances in Catalysis*
2007-	Member of the Hochschulrat, University Duisburg-Essen
2007-	Vice-President of the Deutsche Forschungsgemeinschaft (DFG)
2009-2012	Chairman of the Selection committee of the Communicator Award of the DFG
2009-2012	Vice-Chairman of the Scientific Council of the Max Planck Society
2009-	Vice-Chairman of Dechema
2009-	Member of the Supervisory Board of the Karlsruhe Institute of Technology (KIT)
2010-	Member of the University Council of the University of Oldenburg
2010-	Member of the Trustees of the Federal Institute of Materials Testing and Research (BAM)
2011-	Member of the Board of Trustees of the Award “Otto-Bayer-Preis”
2012-	Member of the selection committee of the “Deutscher Zukunftspreis” (Future Award of the German President)
2012-2015	Chairman of the Scientific Council of the Max-Planck-Society
2013-	Chairman of the selection committee of the “Deutscher Zukunftspreis”

Research in the Department of Heterogeneous Catalysis

The re-direction of the research of the Department of Heterogeneous Catalysis, which had already been mentioned in the last report, continued over the current reporting period and is now more or less complete, although further development is expected also in the future in order to react to new findings and new ideas. Up to about 2010 the prime focus of the Department was the synthesis, characterization and use of micro- and mesoporous materials, supplemented by activities in high throughput experimentation. These research fields have now mainly supporting character, while the focus of the work strongly shifted towards nanostructured catalysts and energy-relevant catalytic processes, for which the former research directions provide an excellent platform to build on. Methodologically, mechanochemistry/mechanocatalysis is playing an increasing cross-sectional role in three different fields: hydrogen storage, biomass conversion, and mechanocatalytical processes under in-situ ball milling conditions.

The new research directions are partly associated also with new group leaders. Roberto Rinaldi had already joined the group towards the end of the last reporting period. His activities are exclusively focused on biomass conversion, with the research on cellulose and mechanocatalytic depolymerization performed in close collaboration with the group of the director Ferdi Schüth. Roberto Rinaldi's activities on lignin conversion, on the other hand, are pursued fully independently. Regina Palkovits had research activities in the Institute in the first phase of the reporting period, although she was formally appointed professor at Aachen University at the end of 2010. Since her laboratories were not ready at that time, her research continued in Mülheim for an appreciable period of time, her last students have finished their experimental work at the end of 2012 in Mülheim. Harun Tüysüz was appointed group leader in 2012, after returning from a post-doc stay in Peidong Yang's group in Berkeley. He is ramping up activities in the field of electro- and photocatalysis with relevance for energy conversion, thus well complementing the activities of Frank Marlow, who has also moved more and more towards photocatalysis over the last years. Wolfgang Schmidt continues his activities in the field of synthesis and applications of zeolitic materials, he was appointed editor-in-chief of the most important journal in this field, Microporous and Mesoporous Materials, in 2013. Claudia Weidenthaler, who had been responsible for powder X-ray diffraction and XPS analysis in the analytical Department headed by Christian Lehmann, was promoted to a group leader position, with dual responsibilities both in pursuing research in the field of in-situ X-ray methods for applications in catalysis and in continuing to provide service in powder XRD and XPS for the Institute.

Michael Felderhoff continues to coordinate the activities in the hydride/hydrogen storage group, which is expanding also in the direction of heat storage. Due to his high international standing, he was appointed member of the hydrogen storage task force of the International Energy Agency.

The research of the Department is multi-facetted, but the core activities lie in the fields of nanostructured catalysts and biomass conversion processes. The division into the different research areas described in the following is to some extent arbitrary, since the activities are closely related and highly integrated. Nevertheless, the subdivision serves to organize the work - at least on a conceptual level – into different directions under a common topic.

Some of the activities described in this report are completely new; some of them continue work along lines established over preceding periods. For instance, in continuation of the activities covered in the last report, a deeper understanding of the solid analogue of the molecular Periana catalyst has been achieved; determination of reaction rates for this highly complex reaction has allowed to benchmark solid catalysts against the molecular system, and activity increase by almost one order of magnitude was achieved. By a wide range of analytical techniques the similarity of the coordination motifs in the solid to the molecular counterpart was proven. A relatively high level of continuity of the work can also be noticed in the synthesis and use of ordered mesoporous materials in catalysis and in the synthesis of gold-based catalysts by colloidal deposition.

While the methods for the production of ordered mesoporous materials are among the core competencies of the Department, this toolbox has been substantially extended: different methods of hard and soft templating are used for the production of catalysts with defined porosity on different levels. These porous matrices, often in the form of hollow spheres, are loaded with catalytically active compounds by different methods, with the goal of producing catalyst particles with precisely defined size and chemical composition. Exemplary important achievements of the reporting period were the production of highly active and very stable electrocatalysts for PEM fuel cells by the novel method of confined space alloying, in cooperation with the group of Karl Mayrhofer (MPI for Iron Research), or the synthesis of carbon-encapsulated PtCo alloy catalysts which allow the synthesis of the fuel molecule dimethylfuran from hydroxymethylfurfural in almost quantitative yield. The second example is also part of the overall activities on biomass conversion. A full process chain, from the mechanochemical depolymerization of native biomass, which incidentally also allows

fractionation of biomass to a cellulosic and a lignin fraction, to the conversion of the celloligomers into value added products, such as hydroxymethylfurfural, sugar alcohols or dimethylfuran, has been developed and covered in a family of patents. Notably, combining three of the processes mentioned, an overall yield of 75 % of dimethylfuran can be achieved in three steps, starting from cellulose. Also the hydrogenation process for the conversion of lignin to liquid hydrogenated products is a highly interesting achievement of the last reporting period.

The entry point into most processes for biomass conversion investigated in the Department is the mechanochemical depolymerization of cellulose and lignocellulosic biomass. This development on the one hand resulted from the experience with milling processes available in the Department, where it had been used over the last ten years as a key method for the synthesis and modification of complex hydride based hydrogen storage materials. On the other hand, the mechanocatalytic work on cellulose and hydride milling has led to transfer of the methodology to heterogeneously catalyzed gas phase reactions. Performing solid-catalyzed gas phase reactions during milling in a ball mill leads to increase in rate by more than three orders of magnitude, an effect which has not been fully understood, yet, but which is a topic of intensive current investigation.

The different groups of the Department are integrated in several bi- or multilateral national and international cooperation networks. These include an EU project on the processing of biooil (Cascatbel), BMBF and AIF grants, integration into the nano-energy program at the University Duisburg-Essen, and participation of the Department in a DFG-Sonderforschungsbereich (collaborative research center). Moreover, in the second funding period of the German Excellence Initiative the Cluster of Excellence (CoE) “Tailor made fuels from biomass” with RWTH Aachen was renewed, with the Schüth and the Rinaldi groups involved, and the CoE “Solvation Science” with the Ruhr-Universität Bochum was funded, also under participation of the Schüth, the Marlow, the Rinaldi and the Tüysüz groups. External funding for the Department was somewhat above 1 M€ per year on average during the reporting period. Integration into these and other scientific networks certainly also helped to advance the careers of several young scientists: Huaiyu Shao was appointed assistant professor in one of the Japanese World Premier Institutes at Kyushu university, Chunjiang Jia became full professor at Shandong University, and Heqing Jiang was appointed full professor at the Qingdao Institute of Bioenergy and Bioprocess Technology of the Chinese Academy of Science.

The members of the Department have been invited to numerous presentations at various institutions and conferences, among them several plenary lectures at important international meetings. Moreover, Ferdi Schüth received several awards, such as the Ruhrpreis für Wissenschaft und Kunst, the Wöhler-Prize of the German Chemical Society (GDCh), the Award of the Hamburg Academy of Arts and Science, the Wilhelm-Klemm-Prize of the GDCh, and the first Chemical Engineering Medal of ETH Zürich. Ferdi Schüth was also active in various capacities beyond the direct research activities. He has served since 2007 as vice-president of DFG, and was re-elected for another three years in 2013. He was also elected as chairman of the Scientific Council of the Max-Planck-Society, and he had a prominent role in the German Academy of Science activities in advising the German government on energy issues. The service of Wolfgang Schmidt as the editor in chief of Microporous and Mesoporous Materials and that of Michael Felderhoff in the International Energy Agency has already been mentioned. Members of the Department, notably Claudia Weidenthaler and many of the Ph.D. students and post-docs, were also very active in outreach activities, especially with the local high schools.

The future research of the Department of heterogeneous catalysis is planned to follow the directions initiated in the past several years, with strong synthetic capabilities as the backbone which serves to support the synthesis of nanostructured catalysts for specific reactions and the activities in the field of biomass conversion. It is expected that the activities directed at understanding the influence of mechanical forces on catalytic reactions will be increased, additionally, research targeted at the exploration of novel feedstocks, such as methane (via syngas) or acetylene, for chemical production is being ramped up. Especially acetylene is considered an attractive molecule, since research on acetylene conversion has been strongly neglected over the last five decades after the decline of Reppe chemistry in times of cheap naphtha feedstocks. With increasing oil prices, acetylene, be it coal based or natural gas based, could become more interesting again, and considering the tremendous progress in catalytic materials, process technology and understanding of catalytic processes, it is expected that new valorization pathways starting from acetylene can be opened.

2.3.1 Research Area "Nanoengineered Catalysts" (F. Schüth)

Involved: M. Feyen, C. Galeano, D. Gu, R. Güttel, C.J. Jia, J. Knossalla, S. Mezzavilla, M. Paul, W. Schmidt, M. Soorholtz, G. Wang, R. Wang, T. Zimmermann

Objective: The goal in this research area is twofold. On the one hand, methodological development is important in order to be able to place desired catalytic functionality at will at desired locations of catalyst materials with compositions freely chosen, on the other hand, these methods are applied for the synthesis of catalysts with high activity and selectivity for specific target reactions.

Results: One of the key synthetic approaches for the production of nanoengineered catalysts is colloidal synthesis.[3,38] This method allows the production of metal or metal oxide particles in solution, where stabilization is typically achieved by capping ligands, such as polymers, fatty acids, or related compounds. These stable nanoparticles can then be further processed in order to produce composite catalysts, or they can be deposited on pre-formed supports, which allows decoupling of the catalyst particle synthesis and the supporting step. Thus, a very high level of control is achieved which allows both fundamental studies and the synthesis of highly interesting catalyst materials.

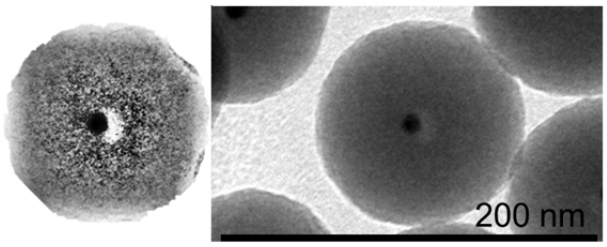

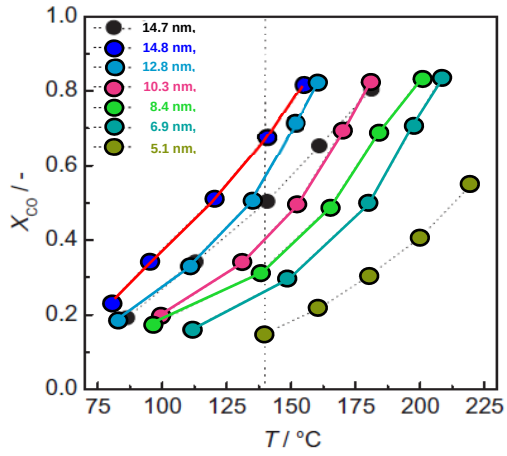

Fig. 1: Encapsulated, partially leached gold particles (top). CO conversion curves for differently sized gold-particle catalysts (bottom). Evaluation of TOFs at 140°C reveal independence of activity on size.

In the last report the synthesis of single gold colloidal particles encapsulated in hollow zirconia shells (Au, @ZrO_2; the nomenclature denotes first the encapsulated species, the blank after the comma indicates that the shell is not directly coated onto the core, and after the "@" the shell material is indicated; possible further shells are indicated by additional "@shell"-levels) had already been described. These materials are highly interesting systems for the study of effects which render

gold colloidal particles active in, for instance, CO-oxidation, since for such systems manipulation of particle sizes and doping levels is possible under precise control of the number of particles present. Such studies were therefore pursued in the reporting period after the synthesis had been well established. By controlled leaching (Fig. 1) it was shown that down to a size of 5 nm, starting from the initial size of 16 nm, the activity per gold surface site is independent of the particle size.[25] Deposition of small amounts of titania on the surface of the colloidal gold particles prior to encapsulation allows studies of the influence that this oxide has on the activity of gold-based catalysts in CO-oxidation.[5] A clear correlation between the titania doping level and the catalytic activity of the composite encapsulated gold catalysts was established which proves that titania enhances the activity, most probably by supplying oxygen species to the gold sites which are active for CO-oxidation.

If iron oxide nanoparticles instead of gold particles are encapsulated in a silica shell (the outer zirconia shell is not required in this case), very stable catalysts for ammonia decomposition, a reaction which can supply high purity hydrogen, can be synthesized.[11] Reference catalysts were produced by leaching the core of FeO_x@SiO_2 particles to produce hollow SiO_2 shells, then identical iron oxide nanoparticles are added again. This results in nominally identical catalysts as for the encapsulated system; however, in the reference catalyst the iron oxide particles are not embedded in the silica shells any more. Using such catalysts in ammonia decomposition at temperatures up to 800 °C revealed improved thermal stability for the encapsulated system.

In fortunate cases, encapsulation of metal or metal alloy nanoparticles can be achieved by simpler pathways (Fig. 2).[47] Polymerization of 2,4-dihydroxybenzoic acid and hexamethylenetetramine (resulting in a polymer resembling resorcinol formaldehyde gel) under hydrothermal conditions leads to the formation of hollow polymer shells. If during polymerization a noble metal salt is added, noble metal particles form in the

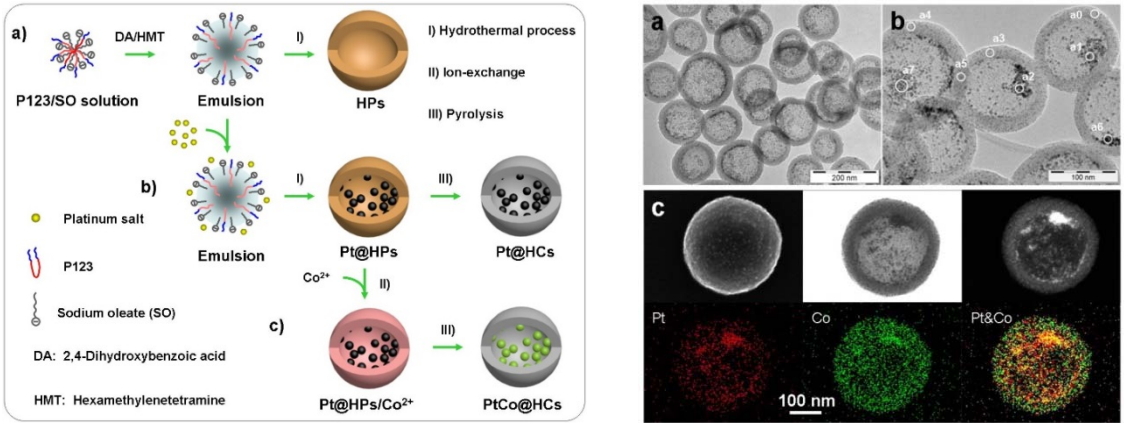

Fig. 2: Schematic synthesis pathway for the production of carbon-encapsulated alloy nanoparticles (left) and TEM, SEM and elemental mappings for encapsulated PtCo nanoparticles (right).

hollow core. Since the carboxylic acid groups in the shell provide ion exchange sites, additional metal components can be exchanged into the catalysts. For many compositions, these exchanged ions migrate into the core and form alloy nanoparticles upon calcination of the polymer shells, while the polymer is transformed into carbon. By controlling the metal concentration in the synthesis, the size of the encapsulated nanoparticles can be controlled. These systems are highly interesting for different catalytic reactions; the PtCo-system allows conversion of 5-hydroxymethylfurfural to dimethylfuran, a very interesting fuel molecule, at almost quantitative yield. In connection with the processes for cellulose depolymerization (see section on cellulose chemistry), this reaction is part of a three step sequence by which 75 % yield of the dimethylfuran fuel can be obtained from cellulose.

Carbon hollow shells are highly interesting not only for the conversion of biomass-derived compounds, but due to its conductivity, it is the support material of choice for fuel cell catalysts. The potential of hollow carbon shell materials for the production of good anode catalysts for PEM fuel cells was thus explored over the last three years. The initial idea was the replacement of the gold core of the Au, @ZrO_2 particles by platinum and to replace the zirconia shell by graphitized carbon. This was found to be possible by a series of nanocasting, leaching, and annealing steps, by which incidentally also the versatility of the synthetic method was demonstrated.[44] As a side result, it could also clearly be proven that carbon is far inferior as a support for gold particles for CO-oxidation compared to different oxides.[12] Since the gold particles are always identical, any differences in catalytic activity can be traced back to the influence of the support, so that the catalysts are ideal model systems. However, the original target, the production of highly active fuel cell catalysts, could not be reached by this approach, since the loading of the catalysts with platinum were much too low for stable shells which need a certain size of approximately 50 nm, while smaller shells, which allow platinum loadings in the 10 % range, are easily destroyed and thus do not provide sufficient stabilization.

The problem could be solved by incorporating the platinum particles not in the hollow center of the spheres, but in the mesopores of the shell itself.[29] With a suitable synthetic protocol, particles with sizes of 1-2 nm could be produced, which only grow to sizes of 3-4 nm after heat treatment at 800 °C, due to the fact that only such particles that are located in the same mesopore coalesce. These hollow graphitic shell based catalysts are excellently suited for application in fuel cells. The major degradation pathways for fuel cell catalysts are particle detachment, growth by Ostwald ripening, and platinum dissolution.[22,27] Encapsulation of the nanoparticles in the carbon matrix suppresses all three deactivation pathways, so that very active catalysts can be

synthesized, which are much more stable compared to conventional, Vulcan-carbon based catalysts, both in accelerated aging tests in rotating disc electrode (RDE) measurements and in real world single fuel cell experiments. In a series of reference experiments with solid spheres having identical pore system and with irregular, bulk mesoporous carbon with identical pore system the superiority of the hollow shell morphology could be proven. It can probably be attributed to better stabilization due to the "quasi 2-D" diffusion pathway, which platinum species have in the shell, and to improved mass transfer due to the hollow core.

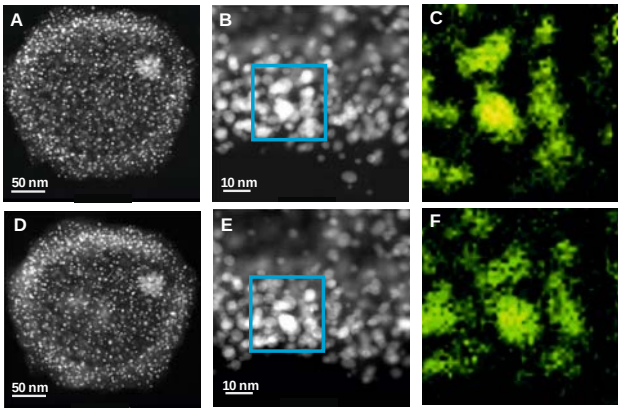

Fig. 3: Identical location TEM images of PtNi loaded hollow graphitic spheres before (top) and after (bottom) accelerated aging test. The elemental map on the left shows the nickel distribution.

This development was very encouraging, but the activity of the catalyst was lower than the DOE target for 2020 which is an important target for work in the fuel cell field. It appears clear that this can only be reached with alloy catalysts, and the work with the stable platinum catalyst inspired the idea of "confined space alloying". The problem with alloy catalysts is the fact that either a high temperature treatment is needed which leads to excessive particle growth, or that preformed alloy nanoparticles are not attached tightly, if they are later supported on a solid, so that rapid detachment occurs. However, the HGS-material provides confining pores, and alloying of individually deposited platinum and nickel precursors should thus proceed without particle growth even after high temperature treatment. The concept was proven for PtNi alloy particles. Stability of this system was so far only demonstraded in RDE measurements, but under the conditions of such experiments, neither substantial particle loss nor particle growth was observed (Fig. 3). However, much more significant is the fact that at least under the RDE conditions the mass activity exceeds the 2020 DOE target by a factor of 2.5 which makes this catalyst system highly attractive. Work is under way to investigate the transferability of the results obtained by RDE experiments to a real single cell under realistic operation conditions. Moreover, a continuous synthesis for the catalyst is being developed in order to render the production scalable.

The nanoengineered systems discussed so far were structured on the scale of several nanometers. However, there is one class of solid catalysts investigated in the Department for which control is exerted at the atomic scale. These are the solid Periana-

type catalysts, which are synthesized by adding a platinum salt to nitrogen-containing porous polymers.[37] Already in the previous reporting period it was shown that Pt-CTF (carbon triazine framework) has activities comparable to the molecular benchmark. This work has now been expanded to other polymers, and the best catalysts outperform the solid Periana system by a factor of almost ten with respect to activity. This precise analysis, however, was only possible because a set-up was built in which reaction rates for this complex reaction system could be measured reliably for the first time. Moreover, by combination of various analytical techniques, including ^{195}Pt MAS NMR, HAADF-STEM and EXAFS, partly at the very limit of what is possible today, with cooperation partners world-wide, it could be proven that the ligand environment in the solid very closely resembles that in the molecular Periana-catalyst, so that one can indeed speak of a solid single-site catalyst.

2.3.2 Research Area "High Surface Area Materials" (F. Schüth)

Involved: D. Gu, C.J. Jia, T. Klasen, I. Lim, V. Nese, Y. Meng, C. Neudeck, A. Padovani, A. Pommerin, F. Richter, M. Ruby, L. Sahraoui, G. Wang, R. Wang

Objective: In this research area, novel methods for the synthesis of high surface area materials, both with ordered and disordered pore systems, are being developed. While in previous reporting periods mostly oxides and carbons were studied, the focus has now strongly shifted to polymeric materials, since these are being explored as catalysts for biomass conversion reactions. The work on high surface area materials is a cross-sectional activity of the Department, with substantial research efforts in the groups of W. Schmidt on zeolitic materials and H. Tüysüz, who investigates ordered mesoporous oxide composites for photochemical and electrochemical reactions. Several projects run jointly with these groups.

Results: Understanding the processes leading to the formation of high surface area materials is a long term research direction in the group. ESI-MS has been developed as a tool to study pre-nucleating solutions.[39] During the last years, it was attempted to extend the systems from silicate systems to $AlPO_4$ and MOF synthesis. In these systems, however, much less pronounced speciation is observed. In the synthesis of $AlPO_4$-18 relatively small units consisting of alternating AlO_4- and PO_4-tetrahedra of up to eleven units were observed. Other than in similar silicate systems, these are clustered with several TEA^+ templating ions, which possibly prevent the formation of higher oligomers. These findings are in line with previous studies, where the formation of $AlPO_4$s via chain and sheet structures has been suggested. Also for the synthesis of the first MOF studied, ZIF-8, condensation to only relatively small units was observed. The kinetics of ZIF-8 formation could be rationalized, since fast precipitation occurs at high imidazolium/Zn ratios, which favors imidazolium incorporation into the oligomers, while at high zinc concentration the addition of zinc is favored.

Zeolites play a major role in several catalysis projects running in the group. The synthesis activities are mostly concentrated in the group of W. Schmidt, but one project on the borderline between high surface area solids and nanoengineered catalysts is also being pursued in the group of F. Schüth. The objective of this project is to elucidate whether the Fischer-Tropsch-synthesis activity of metal particles can be combined with the molecular sieving effect of a zeolite on the level of the zeolite crystallite in order to break the Schulz-Flory-Anderson distribution. This requires the encapsulation of iron

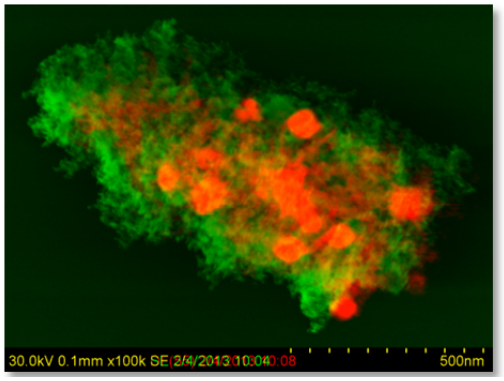

Fig. 1: SEM (green) and STEM (red) overlay of a zeolite particle with embedded iron oxide particles.

nanoparticles within a zeolite crystal which is not possible by directly adding an iron precursor to the zeolite synthesis gel. In that case, the zeolite phase forms as a distinctly separate phase next to the metal oxide, so that the intended effect cannot be exploited. This can be solved by a kind of "stealth" approach. Several years ago the Lyngby group had reported that carbon black particles ("black pearls") can be incorporated in growing zeolites; after calcination, a pronounced mesopore system is generated. If the iron oxide precursor nanoparticles would be covered by a carbon layer, they should be incorporated as well. After optimization of the rather delicate synthesis protocol, this approach proved indeed to be successful. Fig. 1 shows the overlay of an SEM/STEM image which proves the incorporation of the iron oxide nanoparticles in the zeolite. Analysis of the performance in the Fischer-Tropsch reaction is under way.

The synthesis of porous polymers with high surface areas and defined pore structure was one of the key directions of research pursued during the reporting period. The activities range from the synthesis of polymer gels over nanocasting approaches to innovative pathways, i.e. the use of Suzuki-coupling reactions for the direct synthesis of metal loaded polyphenylene. The prototypes of sol-gel porous polymers are resorcinol-formaldehyde composites. Several related compounds have been explored for different applications, but mostly they were used as precursors for high-performance carbons for different applications. The application of such carbons in the conversion of 5-hydroxymethylfurfural to dimethylfuran[47] has already been mentioned in the section on nanoengineered catalysts. A poly(benzoxazine-co-resol)-derived carbon was found to have highly favorable properties for CO_2 capture:[14] it can be obtained in mechanically very stable form, and the nitrogen functionalities introduced in the carbon framework by the addition of amine groups provide excellent adsorption sites for the capture of carbon dioxide. Capacities range up to about 5 mmol/g at 0°C and 1 bar of

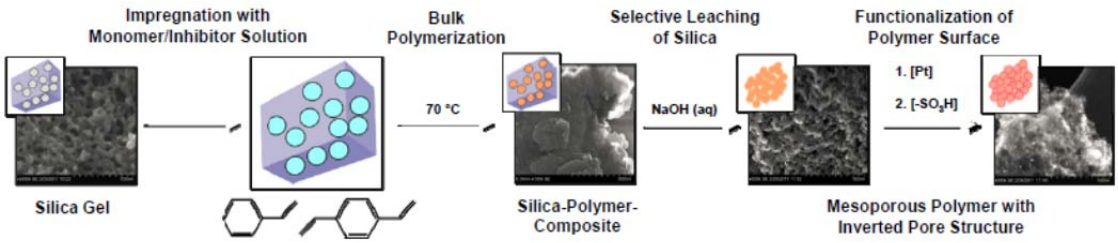

Fig. 2: Schematic representation of the process leading to porous polymer by nanocasting.

CO_2 which are record values for such materials; notably, separation of CO_2 from gas streams is even effective under moist conditions, an advantage which is provided by few sorbents only.

The most intensively studied class of porous polymers were poly(styrene-co-divinylbenzene) which were synthesized by nanocasting.[36,46] Fig. 2 schematically illustrates the process: a porous silica, which can be ordered or disordered, is filled with a polymer precursor, here styrene and divinylbenzene, then polymerization is initiated by a suitable starter. After the polymer has been formed, the silica is leached, typically by treatment with NaOH, then the polymer is ready for subsequent functionalization, which can, amongst others, be sulfonation, metal loading, oxide loading, or others. This method has proven to be extremely versatile. A wide range of different materials, with BET surface areas ranging from a few to about 500 m^2/g and acid site concentrations from about 0.6 to approximately 4.5 mmol/g is accessible by judicious choice of the synthetic parameters.[36] These catalysts proved to be excellently suited for the conversion of fructose to 5-hydroxymethylfurfural. With such a set of catalysts it was also for the first time possible to compare directly the effect of polymeric supports in the oxidation of ethanol to acetic acid and glycerol to glyceric acid against inorganic supports, such as aluminas and carbons.[46] The polymer-based catalysts outperformed the catalysts based on inorganic support: it was generally found that the resin-based catalysts combined the activity of carbon-based catalysts with the selectivity of alumina-based ones.

The most unusual polymer-based catalyst studied was synthesized by a Suzuki-coupling reaction (Fig. 3). This reaction results in a material with a BET equivalent specific surface area of about 1000 m^2/g (the value should be judged with care since the material

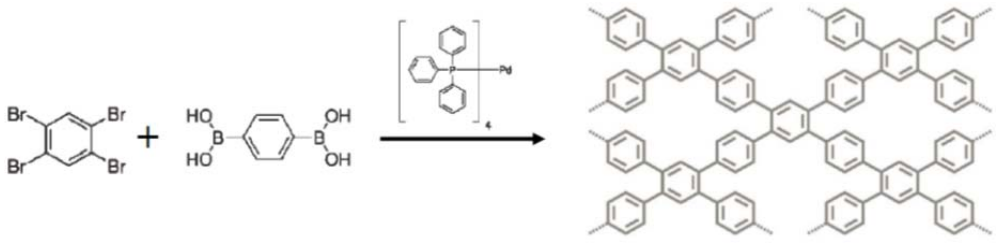

Fig. 3: Reaction scheme for the synthesis of palladium-loaded polyphenylene.

is mostly microporous) onto which at the same time palladium particles with sizes of a few nanometers were deposited. This catalyst, which is synthesized by a Suzuki-coupling, is an excellent catalyst in itself for Suzuki-coupling reactions. More importantly, however, it is one of the most active catalysts for such coupling reactions,

where even sterically highly demanding substrates and chloro-substituted aromatic compounds can be converted at high yields.

While studies into the synthesis of ordered mesoporous oxides are decreasing in importance, there are still very interesting problems to be tackled in this field.[45] These include the synthesis and characterization of composite materials based on ordered mesoporous oxides, and the study of the magnetic properties of such materials.[4] This field was to an appreciable extent developed by H. Tüysüz, while he was still a Ph.D. student in the Department. Now that he is running his own research group, studies in this direction will largely be performed by his team. However, there are a number of projects which were running in the Schüth-group in the reporting period which shall be addressed here.

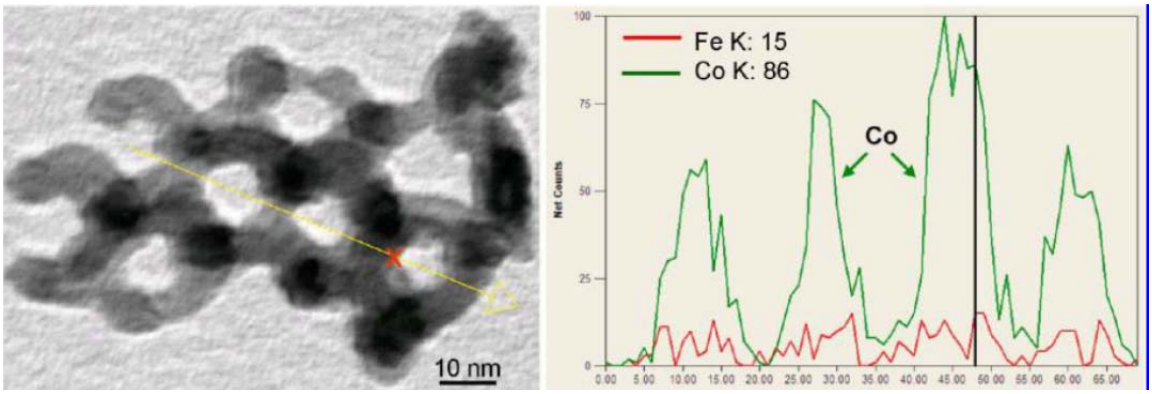

Fig. 4: TEM image of mesostructured $Co_3O_4/CoFe_2O_4$ composite with Ia3d structure (left) and elemental mapping along the yellow line (right), suggesting homogeneous iron and cobalt distribution.

On the synthesis side, methods for the preparation of unusual compositions were further explored. It was thus possible to produce CoO by a careful topotactic reduction of mesostructured Co_3O_4, a method which is not only suitable for cobalt oxides, but can probably be generalized, as shown as a further example for the case of iron oxide.[20] Synthesis of mesostructured CrO_2, a very interesting ferromagnetic material, is still not fully successful, but the CrO_2 content of the mesostructured material could be increased to above 80 %, and we are confident, that further improvements, probably up to the phase-pure material, will be possible. The magnetic properties are the feature which is the reason for exploring these synthetic pathways. Ordered mesoporous oxides provide the opportunity for the creation of magnetic heterostructures. This was exemplified for the case of a hard magnetic $Co_3O_4/CoFe_2O_4$ nanocomposite.[24] Unfortunately, the exact nanostructure – Co_3O_4 with a thin layer of $CoFe_2O_4$ or a mixed crystal – could not fully be elucidated, although the results rather suggest a homogeneous distribution of the iron in the cobalt oxide matrix (Fig. 4). It is hoped that the new electron microscope, which will be delivered in 2014, will help in elucidating the structures in more detail. Such

heterostructures are not only interesting with respect to their magnetic properties (they behave like a homogeneous exchange coupled system), but have potential for photo-electrochemical applications,[49] a research field which is now independently pursued by H. Tüysüz (see corresponding report).

Finally, high surface area Co_3O_4 based materials were also explored as catalysts for CO oxidation. If these materials are doped with small amounts of silicon, they show unprecedented activity for low temperature oxidation, reaching the activity levels of the best gold-based catalysts.[15] This high activity could to some extent be traced back to the influence of the silicon on the size of the cobalt oxide particles,[26] although deeper analysis is still required to fully understand the behavior of the system (see also report of C. Weidenthaler).

2.3.3 Research Area "Novel Catalytic Concepts" (F. Schüth)

Involved: P. Djinovic, R. Eckert, S. Immohr, H. Jiang, W. Schmidt, T. Trotus, D. Wendt, T. Zimmermann

Objective: This group of projects is highly exploratory, since the target is not directly the development of novel catalytic materials or specific conversions, but the investigation of conceptually novel approaches, be it with respect to feedstocks or with respect to the way the reactions are carried out. In previous reports this section had more specific titles, such as "microreaction technology" or "high throughput experimentation", but as long as the concepts explored in this research area are not integrated more into the mainstream of the work of the Department, it is felt that the current title is more appropriate. The topics under this heading are typically investigated only by relatively small groups, on the order of two to three coworkers, in some cases only one coworker is assigned a specific topic.

Results: It is expected that the feedstock situation in the chemical industry will change in the years to come, with a shift from naphtha as the prime carbon source to methane or coal. Both methane and coal can enter the value chains of the chemical industry via syngas or acetylene, and both feedstocks are studied in several exploratory projects. Methane can also be activated by direct oxidation via SO_3, this topic has already been addressed in the section on nanoengineered catalysts.

Syngas has been explored as a feedstock in a number of different – conventional and unconventional – processes. Already in the last and next-to-last reporting periods the activities for the synthesis of methanol and the exploration of the methanol catalyst have been described. The work is now being expanded to the direct synthesis of dimethylether (DME) and oligomethyleneethers (OME). Direct DME synthesis is thermodynamically advantageous compared to the two-step process, in which first methanol is produced and in a subsequent step the methanol is coupled in an acid catalyzed reaction to DME, moreover, for direct DME synthesis a $CO:H_2$ ratio of 1:1 is required which is close to the ratio obtained from biomass gasification and by dry reforming, so that a direct DME synthesis can be coupled to innovative syngas-production routes.

Direct DME synthesis requires the combination of a CO hydrogenation function and an acid function in the catalyst. This can be realized as a mechanical mixture of, for instance, a methanol synthesis catalysts and a zeolite. Such mixtures are effective in

catalyzing the direct synthesis. It has been shown, though, that substantial amounts of carbonaceous deposits form on the catalyst under DME-synthesis conditions. This is strongly suppressed, if a catalyst consisting of a mesoporous γ-aluina loaded with copper nanoparticles is used. This catalysts, however, is somewhat less active and thus requires higher temperatures of reaction.[30] For the zeolite-based catalysts it was found that side products formed at very low concentration in the DME-synthesis reaction, such as ethylene, are the precursor for the carbonaceous deposit. This is not surprising, as olefins are prone to oligomerization and eventually coke formation, and in the methanol-to-olefin reaction a zeolitic component is used in the catalyst. Currently it is studied, how the localization of the CO hydrogenation functionality and the acid function influence the performance of the bifunctional catalyst.

Acetylene is a more unusual alternative feedstock. There are predominantly research activities in Russia and China over the last decades after Reppe chemistry was terminated in most other countries, primarily due to the vast reservoirs of coal.[48] However, acetylene could also be an interesting methane based feedstock, especially in regions with high fractions of intermittent renewable electricity, if acetylene is produced from natural gas in electric arc furnaces. Such systems could have a substantial load levelling influence, since they can be shut down and started up very rapidly. Due to this consideration, activities on acetylene conversion have been ramped up in the Department. This included the commissioning of a compressor system for the supply of high pressure acetylene. This was successful, and acetylene pressures of several ten bar can now be reached routinely in a safe manner. Moreover, an alternative high-pressure acetylene technique was established which consists of dissolving acetylene in a suitable solvent at very low temperature, followed by temperature increase, which results also in acetylene pressures of several ten bar.[48]

Initially, some of the work reported in literature was reproduced as a starting point. Trimerization of acetylene to benzene over niobium chloride could successfully be achieved even below room temperature. Also reaction of acetylene with water and carbon monoxide to result in acrylic acid was found to be possible with the nickel bromide system, which is known from literature. Using palladium acetate, diphenyl-2-pyridylphosphine and an acid with a weakly coordinating anion to catalyze the carbonylation of acetylene to methylacrylate, TOFs as high as $2500h^{-1}$ with above 99% selectivity to the desired product had been reported in literature at a temperature of 50°C. We were able to reproduce these results observing similar activity and selectivity, and also found that supported palladium nanoparticles can catalyze this transformation in the presence of the ligand. We consider this as a first proof of concept, that the reactions of acetylene, which were dominated by homogeneous catalysis in Reppe's

times are also possible over solid catalysts, so that the full tool-box of modern catalysis research can be used to explore novel transformation routes.

A very exciting, thermodynamically possible, transformation of acetylene which, to the best of our knowledge, has not been reported thus far is the reaction with ethylene to form butadiene. Using ruthenium-based metathesis catalysts we were able to show that this transformation can occur via an enyne metathesis reaction. As it is known that in enyne metathesis an excess of ethylene is beneficial, a high excess of ethylene was used, which resulted in a selectivity as high as 43% to butadiene at 93% conversion. Unfortunately, metathesis catalysts can also lead to acetylene polymerization, and generally have TOFs <1000h^{-1}, so that substantial development work is still required in this direction.

Probably one of the most exciting discoveries of the reporting period was the mechanocatalytic rate enhancement by more than three orders of magnitude in the solid-catalyzed CO-oxidation. Milling is a standard technique which is used in the Department in various projects, such as the synthesis of complex hydrides,[16] for quite some time. A first real breakthrough was achieved when the mechanocatalytic depolymerization of cellulose could be demonstrated (see research area "Cellulose Chemistry").[23] This provides a novel and unprecedented entry point into novel biorefinery schemes which has potentially also high commercial value.

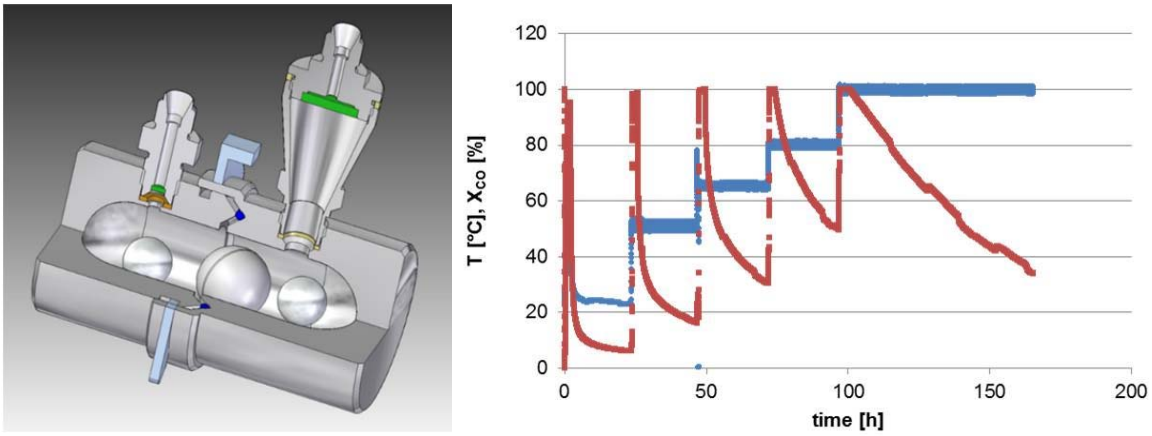

Fig. 1: Schematic drawing of the milling vial (left) and CO conversion at different temperatures during milling and after stopping the mill (right). Conversion jumps to 100 % when the mill is started and decreases after stopping the mill. Catalyst: 1 g gold powder; 50 ml/min 1 % CO in synthetic air.

Inspired by this mechanocatalytic process, the effect of milling on a solid-catalyzed gas-phase reaction was studied. Since there is substantial experience with CO-oxidation in the Department and ready-to-use flow systems were available, this was the first reaction tackled. In order to carry out the reaction under flow-through conditions, a milling vial was constructed which allows such reactions (Fig. 1). Rate enhancement during milling was observed for a number of different catalysts. Most intensively studied were Cr_2O_3

and bulk gold powder. For both systems, rate enhancement by more than three orders of magnitude was observed, which could be clearly traced back to the influence of the milling process by a number of reference experiments.[43] The reason for the enhanced reactivity is not clear, yet. Part of it is probably due to the impact induced hot spots which form between the balls during milling. However, since the activity does not immediately drop down to zero after stopping the mill, but decays over times from minutes to hours, depending on the system (Fig. 1, right), it is probable that milling induced transient defects also contribute to the increased activity. The cause of the rate enhancement is currently under study.

The effect is not confined to CO-oxidation, but is found also for other reactions, such as preferential oxidation of CO in hydrogen-rich gas streams. Moreover, milling can be used to synthesize high activity gold-based catalysts from micrometer sized gold powder, opening up a novel pathway for the synthesis of this class of catalysts which is one of the most intensively studied systems over the last decade.

2.3.4 Research Area "Hydrides for Hydrogen and Energy Storage" (M. Felderhoff, F. Schüth)

Involved: K. Hauschild, D. Krech, K. Peinecke, A. Pommerin, M. Meggouh, R. Schinzel, H.Y. Shao, C. Weidenthaler, B. Zibrowius

Objective: Hydrogen storage materials based on complex hydrides for mobile applications have been in the focus of the group for more than ten years. However, it seems by now clear that the boundary conditions for on-board hydrogen storage in cars cannot be met by such materials.[50] Nevertheless, the work in this direction is continued for two reasons: first, complex hydrides are rather simple, but little explored solids, and thus the exploration of the synthesis, structures, and properties is of interest, irrespective of whether they are immediately useful. Their synthesis, for instance, poses interesting challenges with respect to pressure and temperature range which needs to be realized. Secondly, while complex hydrides and metal hydrides do not appear to have application potential for hydrogen storage, they could be highly suitable as advanced latent heat storage systems, a field that had already been initially explored by B. Bogdanovic in the institute in the 1980s.

Results: After more than a decade of intense research on $NaAlH_4$ doped with transition metals as hydrogen storage material, the actual mechanism of the decomposition and rehydrogenation reaction is still unclear. Early on, monomeric AlH_3 was named as a possible transport shuttle for aluminum, but this compound has never been observed experimentally. It was now for the first time possible to trap the volatile AlH_3 produced during the decomposition of undoped $NaAlH_4$ by an adduct of sodium alanate and crown ether.[50] The resulting $Al_2H_7^-$ anion was identified by solid-state ^{27}Al NMR spectroscopy. Based on this indirect evidence for the formation of the volatile alane, a simple description of the processes occurring during the reversible dehydrogenation of $NaAlH_4$ was possible.

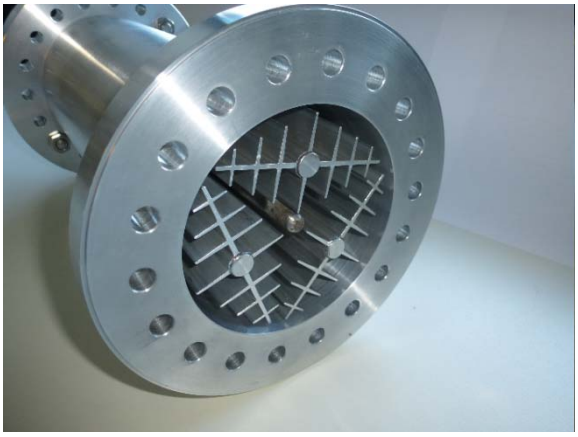

Fig. 1: Prototype of hydride storage tank without the hydride. Fins for cooling are visible.

Even if applications of complex hydrides as storage material for automotive applications appear to be remote, there are other application fields – albeit of smaller scale – where such materials

could be useful. In order to explore the technical implementation of the material in a storage system, a light-weight hydrogen storage tank, charged with Ti-doped sodium aluminum hexahydride Na_3AlH_6, was developed.[13,53] This intermediate hydride has a theoretical hydrogen storage capacity of 3 wt.% and can be operated at lower pressure compared to sodium alanate, $NaAlH_4$. Therefore the tank can be constructed from Al-alloys, with mechanical properties suitable for safe operation of the system. A prototype of the tank is shown in Fig. 1. This prototype was tested under a wide range of pressure and temperature conditions and proved to be suitable for application in combination with high temperature polymer electrolyte fuel cell systems.

Investigations were also extended to other hydrides. Rare earth alanates, such as $Eu(AlH_4)_2$ or the related alkaline earth alanate $Sr(AlH_4)_2$ were studied with respect to structure, thermodynamics and kinetics of the hydrogen release and rehydrogenation.[19] It was found that the decomposition proceeds through an intermediate phase ($EuAlH_5$ and $SrAlH_5$), which, however, is structurally rather different from the hexahydride phase observed in the $NaAlH_4$ system, as could be shown in a combination of powder XRD and solid state NMR spectroscopy. Detailed analysis of both systems revealed – as for most other hydrides – that the thermodynamic properties, but especially the gravimetric storage densities, are insufficient for use in mobile applications. Rehydrogenation of the fully dehydrogenated europium compound could only be achieved to a minor extent, even at pressures of 100 MPa of hydrogen or up to 30 MPa under milling in a pressure ball mill.

MgH_2 is a hydride which has a sufficiently high gravimetric storage capacity of approximately 7.5 wt.%. However, the temperatures for decomposition are too high, the hydrogen is only released above 300 °C. Doping this metal hydride with titanium or other compounds was investigated in order to address both the thermal stability by thermodynamic tailoring due to formation of additional compounds and to improve the kinetic behavior of the system. Direct synthesis via ball milling of magnesium and titanium powder under 30 MPa of hydrogen in a pressure mill allowed the synthesis of a nanostructured MgH_2 doped with TiH_2.[6,16] This composite released hydrogen at temperatures lower by 100°C than bulk-MgH_2, and also rehydrogenation was substantially facilitated. Detailed analysis revealed that the thermodynamic properties of the system are essentially unchanged. For the kinetics the nanostructure is less important than the catalyst, since after several cycles grain growth had occurred, while the positive effect on the kinetics was still observed. This highlights a general problem of nanostructuring hydrogen storage compounds: due to the massive mass transfer during hydrogenation/dehydrogenation cycles the nanostructures are lost in practical

operation, so that special precautions are required to maintain the positive effects of nanostructuring.

Mg-based hydrides are not only interesting for hydrogen storage, but possibly even more useful as heat storage media.[54] Intermediate heat storage for high temperature industrial applications based on thermochemical gas solid reactions possess the highest gravimetric and volumetric energy storage densities of all possible thermal energy storage methods. MgH_2 itself, but also other mixed metal hydrides, such as Mg_2FeH_6 are highly promising for such applications. In particular, Mg_2FeH_6 is suitable for temperatures exceeding 550°C; it is stable over hundreds of cycles and has a volumetric heat storage density of 1500 kWh m^{-3}. Because all experimental results published are based on small lab-scale procedures, we have started a heat storage demonstration project with the development of the tank system, the in- and out-coupling of heat with salt melts and the production of several kg Mg_2FeH_6 as heat storage material. In addition to these technical developments the understanding

$$Mg_2FeH_6 \rightleftharpoons 2\,Mg + Fe + 3\,H_2$$

of the molecular processes during charging and discharging are in the focus of the project. Since such systems have to sustain hundreds or even thousands of cycles in practical applications, full reversibility has to be guaranteed, since otherwise storage capacity will fade. This requires a full understanding of all relevant processes, from the atomic scale up to the level of the grain.

2.3.5 Research Area "Nanostructured Optical Materials" (F. Marlow)

Involved: R. Brinkmann, T.-S. Deng, L. Messmer, M. Muldarisnur, D. Schunk, P. Sharifi, S. Wall

Objective: Novel functional materials consist of a hierarchy of building blocks which have to be assembled by precise and tunable methods. In this research area we investigate fundamental aspects of processing steps, nanostructured building block formation, and the tuning of properties of optical materials.

Results: *Opals.* Nanostructures with length scales in the order of the wavelength of light have specific effects on electromagnetic fields. Photonic crystals (PhCs) are highly ordered versions of them. The self-assembly of these materials, especially of artificial opals, was investigated. The improvement and understanding of one well-defined opal fabrication method developed in this institute was the focus of the research. We found that the opal lattice is strongly aligned in opals fabricated by this method (Fig. 1). This is considered as an important step to mono-crystalline opal films which are, up to now, not existing. The current opal films can be understood as intergrowth structures of two different fcc lattices, each of them interrupted by stacking faults. We found out that the fcc-fcc twinning leads to relatively big domains which are not limiting to potential applications.

The detailed understanding of the opal self-assembly process is another topic of our research. The opal formation can be divided in two temporal phases: the wet assembly and the drying. Both are of different relevance for the quality of the opals. We have followed the second phase by optical spectroscopy in-situ and found significant rearrangement processes during and after water extinction. Optical microscopy, SEM[56], optical spectroscopy[59], and neutron scattering[57,60] have been used for opal film characterization.

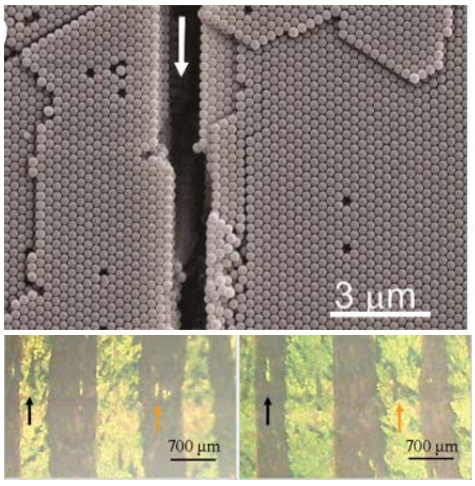

Fig. 1: Opals fabricated by the capillary deposition method (CDM). White arrow: growth direction. SEM images and optical images from two directions.[56, 59]

Core-shell particles. Core-shell particles are interesting building blocks for photonic crystals, catalysis, drug release, and corrosion protection. Their internal structure (shell thickness and composition) can, for example, be used to tune the band structure of PhCs and they are a way to avoid the inversion step which is needed for many PhC applications.[62] Moreover, it turned out that opals made from hollow shells can nearly avoid all cracks. This surprising improvement is ascribed to the enhanced mechanical flexibility of hollow spheres in comparison with solid ones.[65]

NPAs. Nano particle aggregates (NPAs) are also building blocks for photonic crystals, but they can also serve as micro lenses or special scattering particles.[61,63,64] An efficient fabrication method was developed which delivers strongly monodisperse NPAs. Also the shape tuning of NPAs was investigated.

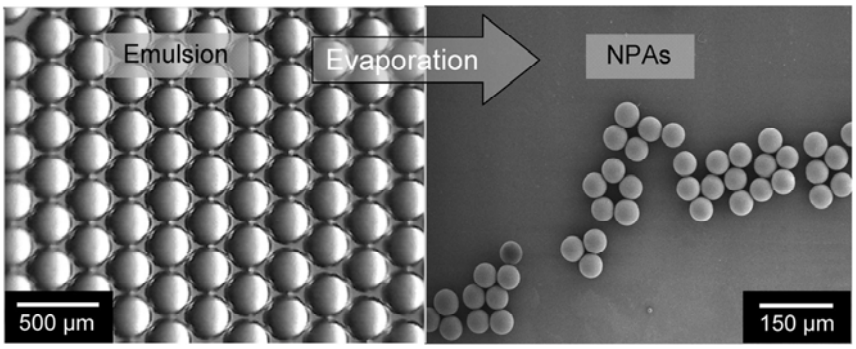

Fig. 2: The NPA fabrication process. The highly monodisperse emulsion is fabricated in a micro fluidic T-junction set-up. The drying leads to the solid NPAs.[61]

DSSCs. Dye-sensitized solar cells are a promising alternative type of solar cells. After 20 years of slow progress with these cells, the interest has increased in the last years again. We also started with works on the fabrication, characterization, and modeling of these solar cells. The key issue is the use of modified semiconductor electrodes and an improved understanding of the charge transport mechanisms in these solar cells.

2.3.6 Research Area "Deep Depolymerization of Lignocelluloses by Mechanocatalysis" (R. Rinaldi and F. Schüth)

Involved: N. Meine, J. Hilgert, M. Käldström, M. D. Kaufman Rechulski

Objective: The utilization of lignocelluloses (*e.g.* wood, grass, crops residues and several others) shows great potential as part of the solution for decreasing the dependence of modern societies on fossil resources. In spite of this, the direct conversion of these renewable carbon sources by chemical and biotechnological processes is hindered by their complex polymeric nature. In plant biomass, three polymers – cellulose, hemicellulose and lignin – form a complex composite that creates the plant cell walls. The composite structure is highly recalcitrant so that chemical or enzymatic processes for hydrolysis of cellulose suffer from low efficacy due to harsh reaction conditions and high byproduct formation in case of the chemical methods, or high costs and long reaction times for the enzymatic methods. Thus, there is an overwhelming need for novel processes to convert the whole plant biomass, forming fermentable sugars and technical sulfur-free lignins. In this group of projects, we aim at the development of energy- and solvent-efficient processes for 'deep' depolymerization, thus leading to full substrate conversion into 'water-soluble lignocellulose.'

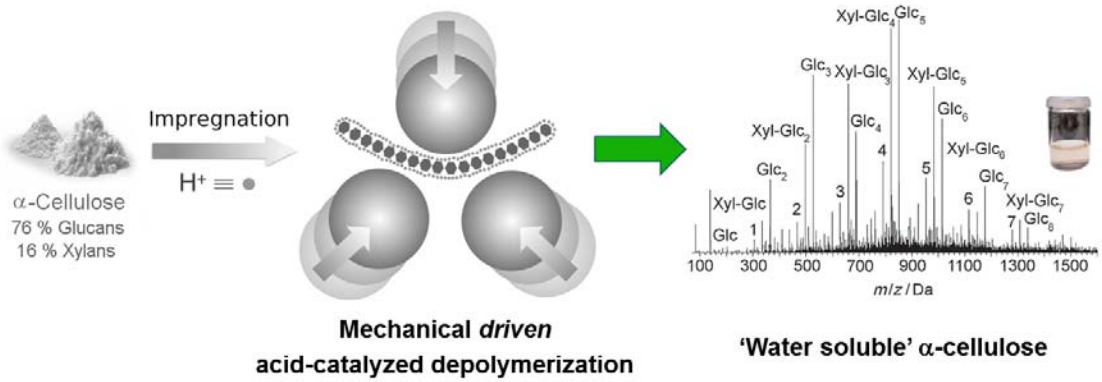

Scheme 1. The pathway towards full conversion of (ligno)cellulosic materials into 'water-soluble lignocellulose.' The substrate is impregnated with catalytic quantities of H_2SO_4 or HCl and then mechanically treated in a planetary ball mill. ESI-MS spectrum of water-soluble products obtained by milling H_2SO_4-impregnated α-cellulose for 2 h. For clarity, products containing a levoglucosan unit (LG) are represented by numbers (n), where the composition is LG-Glc_n. The m/z values correspond to $[M+Na^+]$. Insets show the appearance of products from cellulose.

The real significance of processing 'aqueous solutions of wood', instead of slurries, lies in the prevention of accumulating the highly recalcitrant lignocellulosic residues on

solid catalysts, thus enabling the development of highly efficient processes for biomass valorization by solid catalysts, which is also studied in this area.

Results: Mechanical forces have been exploited for the past few hundreds of years as a first step in wood pulping and conversion of lignocellulose. Usually, conventional mechanical pretreatments (*e.g.* ball milling) are applied to lignocelluloses in order to comminute the substrate and disrupt the crystalline domains of cellulose. As a result, the raw material becomes more amenable for the chemical or biochemical conversions. In fact, moderate hexitol yields (~ 70 %) can be obtained from cellulose conversion in the presence of Ru/C catalysts only, if cellulose is pretreated for 2 to 4 days prior to the catalytic reaction. Similar experiences in other types of conversions (*e.g.* enzymatic saccharification) created a common notion that the effective pretreatment of cellulosic materials by ball milling is always time consuming, and thus very energy intensive for large-scale purposes.

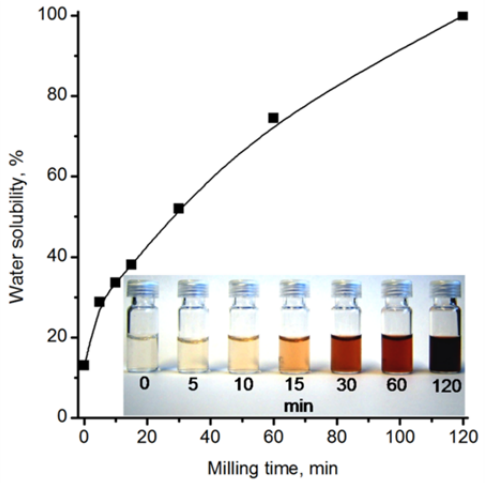

Fig. 1. Formation of water-soluble products (oligosaccharides and lignin fragments) as a function of milling time. Reaction conditions: H_2SO_4-impregnated beechwood (1 g, 0.8 mmol H_2SO_4 per gram of substrate) milled in a planetary mill at 800 rpm for the indicated duration.

'One-pot processes' that combine acid catalysis with mechanical forces thus have not yet been extensively explored for the depolymerization of lignocelluloses. We were the first to demonstrate the full conversion of lignocellulose into 'water- soluble lignocellulose' can easily be achieved by mechanocatalysis within milling durations as short as 2 h.[23] We found that the simple impregnation of substrate fibers with catalytic quantities of a strong acid (e.g. HCl, H_2SO_4) holds the key for the high efficiency. This strategy alleviates the contact problems faced by the experiments performed in the presence of a solid acid. As a result, water-soluble oligosaccharides are formed in quantitative yield within milling duration of 2 h. Most interestingly, lignocellulosic substrates (e.g. sugarcane bagasse, beechwood, pinewood) are also fully converted into 'water-soluble lignocelluloses' within 2 to 3 h (Fig. 1). Remarkably, the method also solubilizes lignin, giving a red-brownish color to the solution products obtained from beechwood (Fig. 1).

Because the mechanical process does not destroy the acid catalyst, no additional acid is required in a subsequent step (taking place in aqueous phase) to hydrolyze the soluble

oligosaccharides. This fact offers an attractive and inexpensive alternative to enzymatic hydrolysis. In fact, oligosaccharides undergo hydrolysis at temperatures as low as 130 °C for 1 h, forming 91 % glucose, 8 % glucose dimers and 1 % HMF relative to the glucan fraction, and 96 % xylose and 4 % furfural relative to the xylan fraction.[23] Such high yields in monosaccharides with such a low degree of byproduct formation using such a simple process are unprecedented.

Even more impressive are the results for the saccharification of 'water-soluble beechwood. The reaction starting with a 10 wt% aqueous solution of depolymerized beechwood (pH 1, at 140 °C for 1 h) also resulted in high yields of monosaccharides (84 % glucose and 89 % xylose, relative to the glucan and xylan fractions, respectively). However, the saccharification led to an unexpected result – the precipitation of a *sulfur-free* lignin (Fig. 2). The separation of lignin from the monosaccharide solution becomes thus feasible by simple filtration.

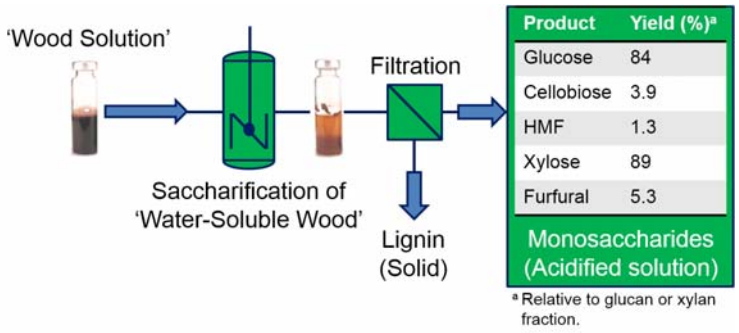

Fig. 2. Fractionation of beechwood into fermentable sugars and sulfur-free lignin by saccharification of 'water-soluble beechwood.'

The absence of sulfur in these lignin precipitates distinguishes these materials from technical lignins obtained by current pulping processes (*e.g.* kraft and sulfite processes, which may contain up to 10 wt.% sulfur). Furthermore, it is conducive to advanced utilization of the lignin precipitates for the production of high value products (*e.g.* chemicals, fuel additives and carbon fibers).

We also demonstrated the deep deploy-merization as a unique entry-point process for efficient production of sugar alcohols from cellulosic substrates.[34] Under low-severity

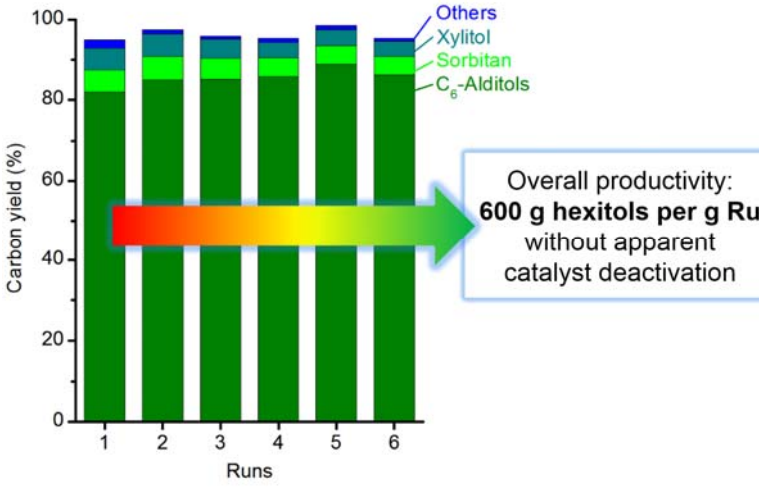

Fig. 3. Recycling of Ru/C. Reaction conditions: 500 mg depolymerized microcrystalline cellulose, 10 mL water, 100 mg Ru/C, 50 bar H_2 (r.t.), at 160 °C for 1 h.

conditions, 94 % yield of hexitols was obtained from the depolymerized microcrystalline cellulose, in the presence of a pre-activated Ru/C, by a batch reaction at 150 °C for 1 h. Noteworthy, such a high yield was achieved in an overall time of only 3 h, that is, *24-36 times faster* than the best examples reported so far. Indeed, a commercial Ru/C catalyst was fully compatible with the presence of H_2SO_4 in the reaction medium. The catalytic activity of Ru/C was fully maintained throughout six runs at 160 °C for 1 h each, as seen in Fig. 3. In the recycling experiments, the cumulative productivity achieved about 600 g of hexitols per g of Ru. As the catalyst is still highly active at the sixth reaction run, this value will be much higher in an extended recycling test.

In a joint research project with J. A. Dumesic (U. Madison-Wisconsin), we also demonstrated the high-yield production of furfurals starting with mechanocatalytically depolymerized substrates.[41] This reaction is conducted in a biphasic reactor containing an organic phase (4-propylguaiacol) and an aqueous salt phase comprising the sugar oligomers. Short reaction times are possible with the use of microwave heating and limit the extent of degradation reactions. Remarkably, at a conversion of glucans of 94% or higher, the isolated yield of HMF reached 60 and 69% in the experiments beginning with water-soluble products from beechwood and sugar cane bagasse, respectively. These yields are remarkably high, as similar studies have reported HMF yields of ~35% when starting from pinewood. Full conversion of xylose with high selectivity for furfural was achieved for the lignin-containing substrates. Again, the current yields of furfural (74 – 84 %) are also higher than those previously reported for the direct processing of solid lignocellulosic substrates (~ 65 %).

One may argue that milling would not be a feasible solution on the scale required for bulk processing of lignocellulosic biomass. Amidst the several conditions studied for the mechanocatalytic depolymerization, we found good correlations of the estimated energy dose, transferred to the substrate, with the achieved solubility of the products. Table 1 compares the milling energy input required for full conversion of the substrate into water-soluble products with the substrate energy content. Most importantly, we have found that the method would be, indeed, already feasible on a kilogram-scale, as indicated by the lower energy demand of the method (by a factor of 0.3-0.7) relative to the substrate energy content.

Table 1. Comparison of the energy demand for the milling process at several method scales.

Method scale (g)	Milling energy input / substrate energy content*
2	49
40	7
100	1
1000	0.3-0.7

* Values estimated considering an average energy content of dry wood of 18 MJ/kg.

2.3.7 Research Area "New Catalytic Methodologies for Valorization of Lignin" (R. Rinaldi)

Involved: X. Wang, P. Ferrini, G. Calvaruso, N. Ji, H. J. Estevez-Riveira, J. Geboers

Objective: Lignin occurs alongside hemicellulose and cellulose in the plant cell walls. Chemically, lignin is a network polymer made of phenylpropenyl units (*i.e.* coumaryl, syringyl and coniferyl alcohols) that are randomly connected by C—C and C—O bonds (Scheme 1). This biopolymer corresponds to up to 30 % of the plant biomass composition and 40 % of the energy content of lignocellulose. Hence, to find outlets for technical lignins is clearly required for lignocellulose utilization to become carbon economic and energy efficient. At the first sight, the structural model of a native lignin suggests that this feedstock could serve as a raw material for the production of phenols. In this context, hydrogenolysis of aryl alkyl ethers is a reaction receiving increasing attention because of the large fraction of lignin subunits connected by such ether bonds (Scheme 1). However, the lack of catalytic methodologies able to transform the polymeric lignin into solely a class of monomeric products present a major barrier to exploit the potential of this feedstock to the fullest. In this group of projects, we aim to establish a world-class laboratory on catalysis for lignin valorization. The mission of this laboratory, supported by the Alexander von Humboldt Foundation through the Sofja Kovalevskaja Award 2010 given to Rinaldi, is to contribute to the foundations for the rational design of catalytic systems for efficient lignin conversion. Accordingly, we rely on two main strategies to develop catalysis for lignin conversion. First, to understand the solvent effects on the hydrogenolysis/hydrogenation of lignin in the presence of Raney Ni and other Ni catalysts. Second, to design reaction pathways for the molecular simplification of lignin feeds (organosolv lignin and biogenic phenols from bio-oil) based on catalytic hydrogen transfer.

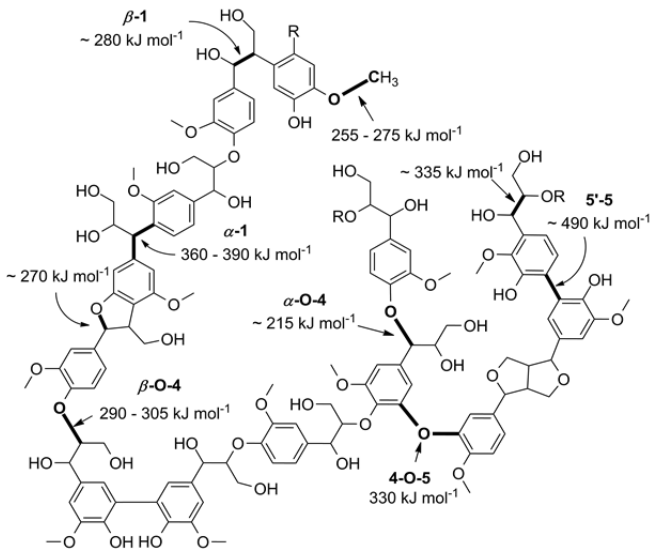

Scheme 1. Example of lignin structure depicting some of the primary inter-unit linkages and the corresponding average values of bond dissociation enthalpy.

Results: Solvents play an important role in catalytic hydrogenations. So far, however, there has been almost no discussion on the influence of solvents in the catalytic hydrogenolysis of lignin or related model compounds. Aiming to ultimately assess the solvent effects on the hydrogenolysis of lignin, we first examined the influence of several solvents in a model reaction using diphenyl ether, a substrate comprising a very strong C–O bond (analogous to 4-O-5, Scheme 1). In the exploratory study, Raney Ni was chosen for several reasons. Unlike noble metals, which show usually a high chemoselectivity towards hydrogenation or hydrogenolysis, Raney Ni is a relatively less expensive material and a 'promiscuous' catalyst in regard to its chemoselectivity. Hence, Raney Ni is able to tackle the structural complexity of lignin, thus showing great potential for lignin conversion.

As expressed by a solvent parameter called 'donor number', the Lewis basicity of the solvent was identified as one of the most important parameters accounting for the activity and selectivity of Raney Ni in the conversion of diphenyl ether. In non-basic solvents (*e.g.* 1,1,1,3,3,3-hexafluoro-2-propanol and alkanes), Raney Ni is an extremely active catalyst for hydrogenolysis and hydrogenation, as shown by the full conversion of diphenyl ether into saturated products. In basic solvents, however, Raney Ni is less active, but a much more selective catalyst for hydrogenolysis of the C—O bonds.

Lignin conversion can be performed even in solvents in which lignin is insoluble. Indeed, lignin starts to undergo thermolysis at temperatures as low as 160 °C. This non-catalyzed process brings aromatic fragments into solution and, consequently, enables the action of solid catalysts. Nonetheless, for high conversion of solid lignin, the process should be performed at temperatures above 250 °C, although such a requirement increases the energy demand of the process. We found that subjecting organosolv lignin to Raney Ni in methanol under an initial H_2 pressure of 7 MPa *(r.t.)* at 300 °C for 8 h is an effective strategy to produce a complex mixture of phenols from lignin. In turn, if saturates are the desired products, solvents possessing no Lewis basicity (*e.g.* methylcyclohexane) are the best choices for the lignin conversion.[71]

Raney Ni is able to catalyze the reduction of many organic functionalities by transfer hydrogenation using 2-propanol as an H-donor. These reactions usually take place under reflux conditions. The transfer hydrogenations with Raney Ni have not

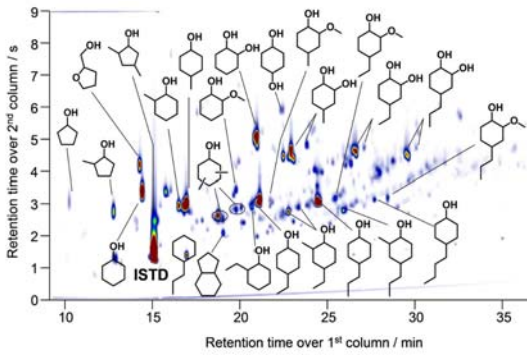

Fig. 2. GC×GC image of bio-oil processed by transfer hydrodeoxygenation using 2-propanol as solvent and H-donor at 160 °C for 3 h.

found extensive uses in organic synthesis due to the lack of chemoselectivity, very often leading to defunctionalization of complex molecules. This 'disadvantage' attracted our attention because the upgrade of highly functionalized phenols, such as those found for the lignin substructures or bio-oil, requires catalysts capable of simultaneously reducing several functionalities under low-severity conditions.

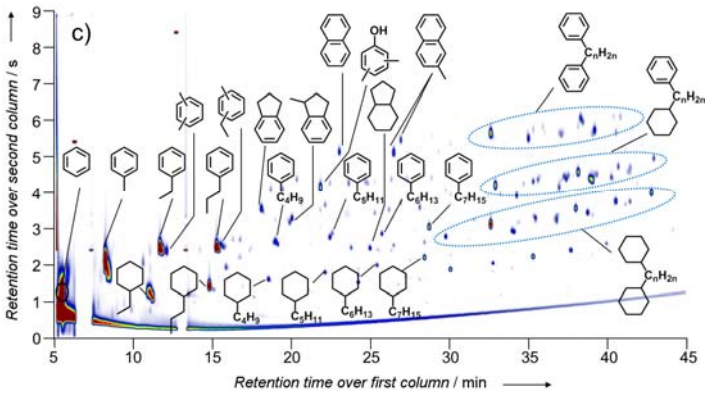

Fig. 3. GC×GC-MS of lignin products obtained from the tandem dehydroxylation of phenols. Reaction conditions: Raney Ni (0.6 g), H-BEA-35 (0.050 g), substrate (0.1 g), 2-PrOH (0.50 g), *n*-pentane (7 mL) processed at 160 °C for 2 h and sequentially at 240 °C for an additional 2 h.

We demonstrated the transfer hydrodeoxygenation of the phenolic fraction of bio-oil to a mixture of cyclic alcohols and diols to be feasible under unprecedented low-severity conditions (*e.g.* 160 °C and autogeneous pressure).[70] In spite of the importance of the aforementioned findings, we realized that the even in the best cases, the formation of mixtures of oxygenated products from lignin (*e.g.* phenols, cyclohexanols and cyclohexanones) still does not suffice for utilization of lignin by the chemical industry. This is because the cracking of the complex structure of lignin leads to very complex product mixtures having only low content of individual components. In effect, since the oxygenated lignin products have high boiling points (*e.g.* phenol, 182 °C), the product separation is very difficult to envision on such a large scale as needed for the lignocellulosic biorefinery. Thus, the complex mixture of oxygenated products would be mostly destined for low-value purposes. Alternatively, the conversion of lignin yielding

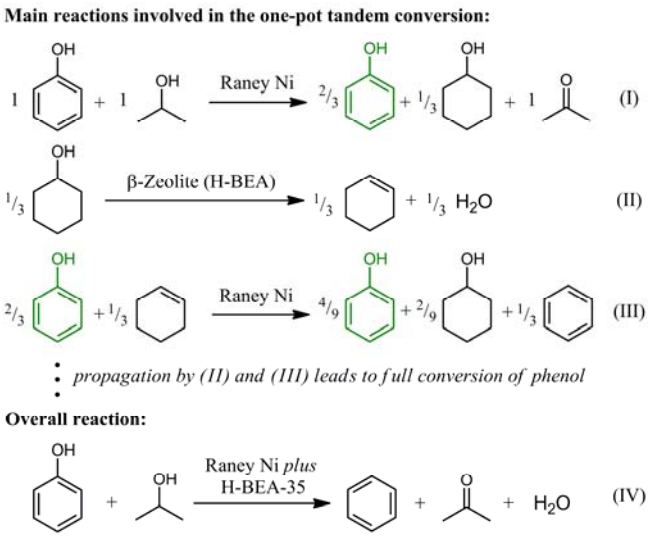

Scheme 2. Simplified pathway for the dehydroxylation of phenols to arenes by catalytic tandem reactions with concurrent use of Raney Ni and β-zeolite (H-BEA-35). The structure in *green* corresponds to the unconsumed phenol by (I) and (III).

arenes with low boiling point could greatly facilitate the fractionation and further processing of the arene mixtures into chemical commodities (*e.g.* benzene, toluene, ethylbenzene and xylenes) by conventional refinery and petrochemical routes.
In spite of the potential in lignin and bio-oil valorization, the dehydroxylation of phenols is a very challenging chemical transformation. In fact, the Ar—OH bond has a bond dissociation enthalpy of 465 $kJ \cdot mol^{-1}$, which is even higher than that of a C—H bond in methane (439 $kJ \cdot mol^{-1}$). In organic synthesis, there are few methods available for phenol dehydroxylation. Typically, they require the derivatization of the Ar-OH group with an electron withdrawing group for weakening the C—O bond. As such, the derivatization enables the hydrogenolysis of the C—O bond with the use of Pd/C and H_2, thus forming the corresponding arenes. It is understandably difficult to envision the utilization of these procedures on a large scale, since they generate stoichiometric quantities of waste.

We demonstrated a novel pathway as highly useful for the depolymerization of lignin and removal of its oxygen-containing functionalities in addition to dehydroxylation of phenols.[73] The novel approach for phenol dehydroxylation (Scheme 2) consists in coupling (I) hydrogenation of phenol to cyclohexanol and (II) dehydration of cyclohexanol to cyclohexene with (III) dehydrogenation of cyclohexene to benzene. Under H_2 pressure, the combination of steps (I) and (III) in a one-pot procedure is impossible. However, steps (I) and (III) become compatible in a one-pot procedure when the reactions are performed by *H-transfer in the absence of* H_2. The conversion of phenol continues by the utilization of cyclohexene formed by (II) because the reaction (III) is thermodynamically more favorable than (I). Therefore, the formation of arenes occurs by the propagation of the reaction chain by (II) and (III). The one-pot procedure is carried out in the presence of Raney Ni and β-zeolite using 2-propanol solely as a starting H-donor, that is, in a molar ratio 2-propanol-to-phenol below 3. Applying the catalytic procedure to organosolv lignin (Fig. 3) resulted in an isolated yield of about 40 wt% colorless oil (78 % of the detected products are arenes, 18 % alkanes, and only 4 % are phenols). Similar results were obtained from the upgrade of the phenolic fraction of bio-oil. Overall, if one considers that the lignin has 70 % of C-content, and the products, 80 - 90 %, isolated yields of ca. 50 % corresponds to a very good carbon yield of *ca.* 70 - 80 %.
In conclusion, the unprecedented high selectivity to arenes obtained under low-severity conditions provides a new route in stark contrast to emerging approaches for catalytic upgrade of bio-oil or other methods using H-transfer which are performed under extremely harsh conditions (5 – 20 MPa, 300 – 500 °C). Finally, even if the isolated

yield of the products is insufficient to give a suitable return in today's chemical industry, the mixture of arenes and aliphatics could very well serve as valuable bio-additives to synthetic fuels produced by the Fischer-Tropsch process, which lack aromatic and branched hydrocarbons required for high-performance of fuels for aviation or Otto-engines.

2.3.8 Research Area "Understanding the Mechanisms of Dissolution and Hydrolysis of Cellulose in Electrolytes" (R. Rinaldi)

Involved: H. F. Nunes de Oliveira, A. Carvalho, N. Meine

Objective: Native cellulose is, for several reasons, often unsuitable for technical applications. Accordingly, the dissolution of cellulose is essential to reshape the natural fibers, thus providing materials with the desired properties. Furthermore, in solution, cellulose is not physically protected by its supramolecular structures, thus enabling the direct investigation of its chemical reactivity. In this group of projects, research into new solvents for cellulose and mechanisms of cellulose dissolution and hydrolysis have been performed.[75]

Results: In 2011, a significant breakthrough was achieved by us,[67] we introduced a novel class of solvent systems for cellulose (Fig. 1). We demonstrated organic electrolyte solutions, which contain just a minor mole fraction of ionic liquid (χ_{IL}), as better solvents for cellulose than the parent ionic liquids (ILs) themselves. These solutions are able to instantaneously dissolve cellulose in concentrations as high as 25 wt%. This striking finding overcomes the major drawbacks that the dissolution of cellulose in neat ILs faces (*i.e.* the slow rate of dissolution, the high viscosity of the solutions obtained, the limited solubility of cellulose and not to mention the high costs of ILs). Indeed, the dissolution of cellulose in neat 1-butyl-3-methylimidazolium chloride (BMIMCl) is a process well-known to take more than 10 h.

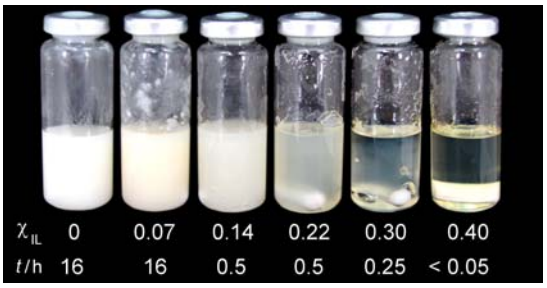

Fig. 1. Appearance of the mixtures containing microcrystalline cellulose (Avicel, 10 wt %), 1,3-dimethyl-2-imidazolidinone and 1-butyl-3-methyl-imidazolium chloride after stirring at 100 °C for the time indicated in the figure. Note that there is a magnetic bar at the bottom of the vials.

Upon dissolving easily 10 wt% cellulose in few minutes (Fig. 1), the simultaneous use of BMIMCl and 1,3-dimethyl-2-imidazolidinone (DMI) brought enormous benefit to the process. Moreover, the use of 1-ethyl-3-methylimid-azolium acetate (EMIMAcO) as IL in the solvent system allows instantaneous dissolution of cellulose at 100 °C. This feature enabled the determination of $\chi_{EMIMAcO}$ at which the dissolution of cellulose was achieved in the molecular solvents at 100 °C (Fig. 2).

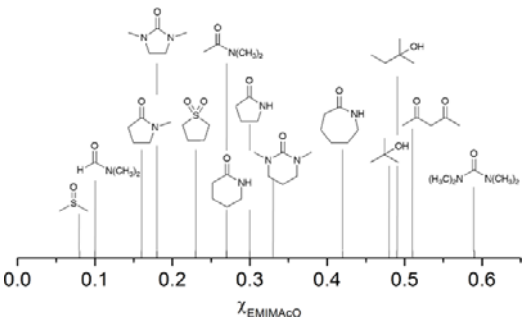

Fig. 2. Mole fraction of 1-ethyl-3-methyl-imidazolium acetate ($\chi_{EMIMAcO}$) required for the instantaneous dissolution of Avicel in several molecular solvents at 100 °C.

As we demonstrated in several contributions published in 2008-2010, the supramolecular structure of cellulose is fully disassembled upon dissolving the biopolymer in ILs, and as a result, cellulose displays reactivity similar to cellobiose. Nonetheless, even in solution, the hydrolysis of 1,4-*β*-glucans needs a strong acid catalyst ($pK_a \leq 3$) to proceed at reasonable reaction rates. This fact suggests that there should be other factors contributing to the high resistance of 1,4-*β*-glucans to hydrolysis.

In the period from 2011-2013, we have been working on a fruitful joint project with AK Thiel. We explored the electronic structure of cellobiose by DFT at the BB1K/6-31++ G(d,p) level.[74] The predictions suggest that cellulose is protected against hydrolysis not only by its supramolecular structure, as currently accepted, but also by its electronic structure, in which the anomeric effect plays a key role. The DFT studies provide very important insights on the hurdles that hydrolysis of cellulose faces (Fig. 3):

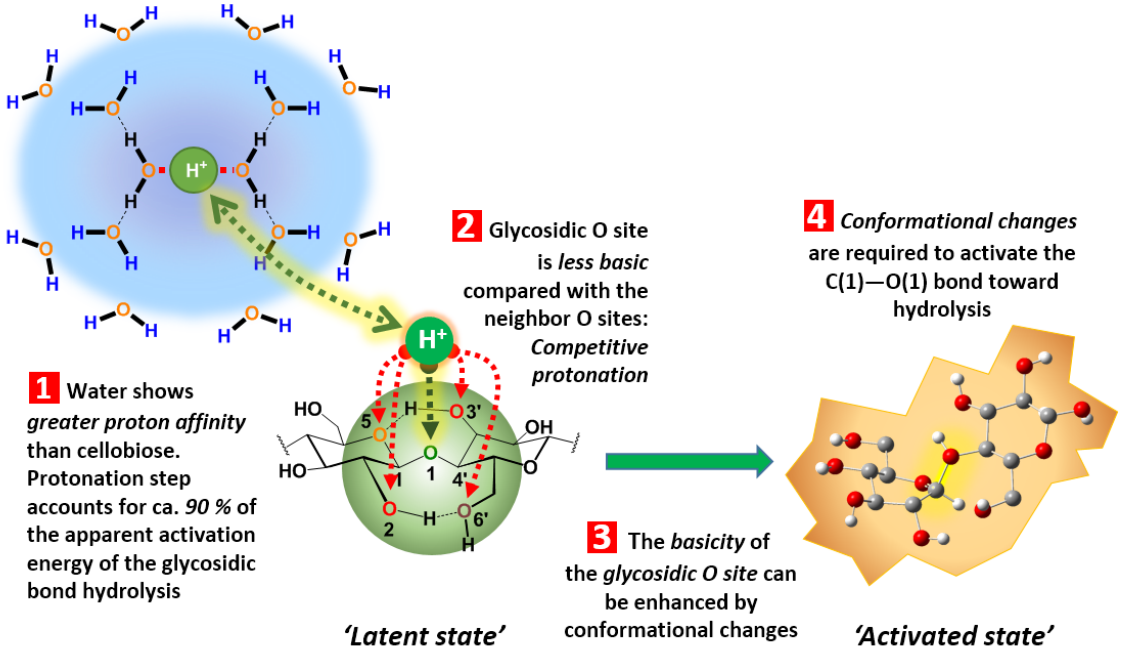

Fig. 3. Overcoming the chemical barriers of cellulose hydrolysis by mechanocatalysis.

These DFT predictions also shed light on the results recently reported for the solvent-free, mechanocatalytic depolymerization of cellulose, in which the biopolymer can be

fully converted into water-soluble oligosaccharides in the presence of a strong acid. The general mechanistic aspects of the hydrolysis of cellobiose strongly suggest that the hydrolysis of cellulose depends heavily upon conformational changes. Accordingly, we propose that mechanical forces serve to activate the ‘latent state’, i.e. the protonated cellobiose subunits occurring in the cellulosic chain, thus inducing the required conformational changes for the cleavage of the glycosidic linkage. Nonetheless, the reaction still requires a strong acid, which is conveniently provided by impregnation of cellulose with H_2SO_4 or HCl. Indeed, milling cellulose without additives leads mainly to the destruction of the crystalline domains. In this case, there is only little depolymerization, with very low yields of water-soluble products.

2.3.9. Research Area "Formation of Nanoporous Silicates" (W. Schmidt)

Involved: X. Gu, M. Castro, I. Lim

Objective

Nanoporous silicates possess pores with sizes equivalent to molecular dimensions and serve as molecular sieves and selective catalysts in various applications. Pore diameters as well as pore shapes and pore organization determine the interaction with molecules from fluid phases. Crucial factors that affect the properties of such materials are composition, pore sizes, particle sizes and morphologies. They determine adsorptive and diffusional properties as well as catalytic activity. Understanding the formation processes of nanoporous silicates is subject of this research area.

Results: Zeolites are well known adsorbents and highly efficient catalysts in petrochemistry. Nevertheless, their nucleation and crystallization processes remain still not well understood. The formation of early silicate species in the crystallization of zeolites has been investigated by a combination of liquid state ^{29}Si, ^{27}Al, and ^{1}H nuclear magnetic resonance (NMR) spectroscopy, small angle X-ray scattering (SAXS), dynamic light scattering (DLS) and electrospray ionization mass spectroscopy (ESI MS) in collaborations with colleagues from the Universities of Versailles, France, and Leuven, Belgium.

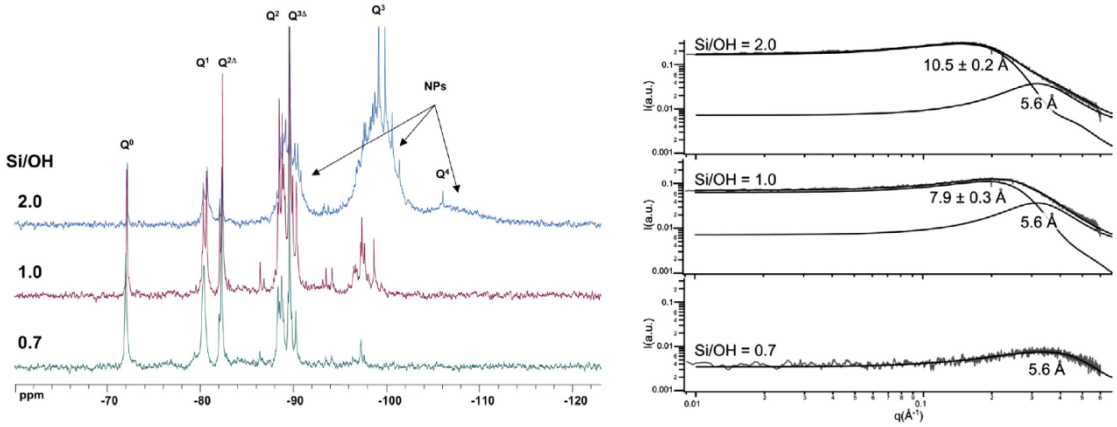

Fig.1. ^{29}Si NMR spectra (left) and SAXS data (right) measured on synthesis mixtures for zeolite beta with different Si/OH ratios prior to heating of the solutions (particle radii are given under the SAXS curves).[83]

Starting from clear reaction solutions with tetraethylammonium hydroxide (TEAOH) as the structure directing template, the silicate speciation has been monitored [83]. The appearance of nanoparticles, indicated by very broad NMR signals, depends strongly on the Si/OH ratio of the reaction mixture as illustrated in Fig. 1. At low Si/OH ratios, no nanoparticles are observed in reaction mixtures prior to hydrothermal reaction whereas at Si/OH > 1 nanoparticles are observed already at room temperature. The NMR line broadening is caused by restriction of the rotational freedom of the silicate species in the emerging solid particles. These observations are corroborated by ESI MS, DLS, and SAXS data. The SAXS curves, as shown in Fig. 1, can be modeled by populations of spherical nanoparticles. In addition, SAXS reveals individual silicate species with sizes of about 1 nm for solutions with Si/OH <1. They can be either larger silicate oligomers or very small silicate nanoparticles that also condense into amorphous nanoparticles upon hydrothermal treatment. ^{1}H NMR and ^{27}Al NMR reveals that the amorphous nanoparticles contain a fraction of the structure directing agent tetraethylammonium hydroxide (TEAOH) and all aluminum present in the reaction mixture. Crystallization of zeolite beta upon hydrothermal heating proceeds then from the amorphous particles and nucleation of the zeolite appears to proceed on the silicate nanoparticles.

Mixing of tetraalkylammonium molecules with an amphiphilic template results in mesoporous silicate with microporous pore walls. That has been investigated in collaboration with the colleagues from the Ruhr University in Bochum. Precursor solutions with tetrapropylammonium hydroxide (TPAOH) have been synthesized and mixed with solutions containing cetyltrimethylammonium bromide (CTAB). In contrast to conventional ordered mesoporous silicates such as MCM-41 and MCM-48, the resulting materials possess microporous walls as could be shown by a combination of analysis techniques, including wide and low angle XRD, adsorption studies, and ^{129}Xe NMR spectroscopy[81]. Analysis of the pair distribution function (PDF) of high resolution XRD data showed that the structure of the silica in the pore walls resembles that of MFI zeolites even though no distinct XRD reflections are observed.

Using the same combination of CTAB and TPAOH in combination with NaF as mineralizing agent, ordered mesoporous aluminosilicate (OMA) with exceptional hydrothermal stability could be synthesized in our laboratory. Structural integrity is maintained in boiling water for at least 5 days as well as upon exposure to water vapor at 600°C for a couple of hours [78]. The silica is formed as spherical particles within radial mesopores (Fig. 2 left) and a large fraction of the aluminium in the pore walls was found to be coordinated tetrahedrally (54 ppm signal in ^{27}Al MAS NMR spectrum, Fig. 2 right). Only a smaller fraction is found in octahedral coordination (signal at 0 ppm). The IR spectrum of pyridin adsorbed on that aluminosilicate showed signals

typical for both, Bronsted and Lewis acid sites, indicating that the obtained aluminosilicate probably also contained structural units similar to those in the MFI zeolite.

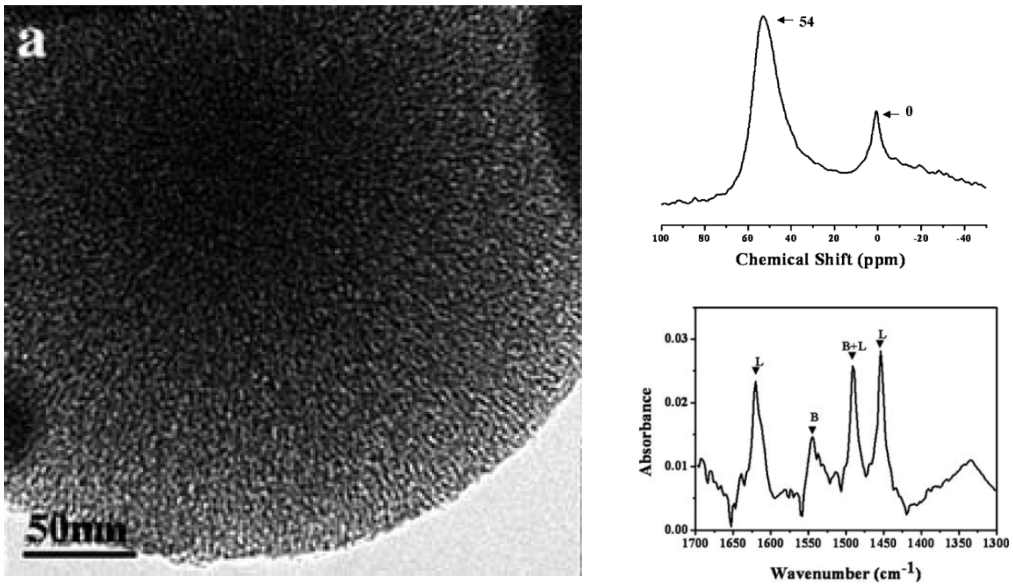

Fig. 2. TEM image of radial channels in ordered mesoporous aluminosilica from CTAB-TPAOH-NaF system (left) and ^{27}Al MAS NMR spectrum (top right) and IR spectrum of adsorbed pyridine (bottom right). [78]

Benzylation of toluene with benzyl alcohol is catalyzed by Bronsted acid sites and the OMA showed more or less quantitative conversion and high selectivity to benzyl toluene (S_{BT} > 70%) whereas commercial ZSM-5 mainly produced benzyl ether (S_{BE} > 90%) at very moderate conversion (C_{BzOH} < 5%). The large mesopores in OMA promote mass transfer and the acidity of the aluminosilicate facilitates the benzylation of toluene.

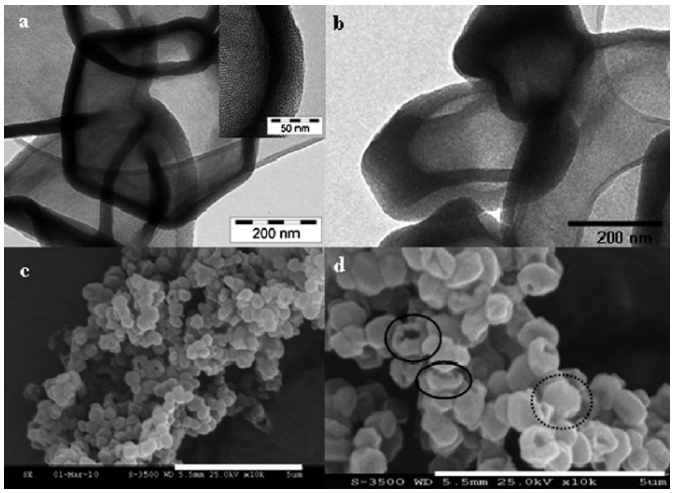

Fig. 3. TEM and SEM images of hollow mesoporous aluminosilicates. [79]

Replacing TPAOH by NaOH in the same reaction mixture as used for the synthesis of the OMA, hollow aluminosilica polyhedra with very thin walls are formed as he hollow polyhedra depends on the thermal reaction at 140°C, the solid

phase is MCM-41 and consists of particles with similar shapes as the final products. The hollow cores are formed during hydrothermal treatment of the aluminosilicate particles. The aluminum-rich outer rims of the MCM-41 particles withstand dissolution whereas the siliceous centers are dissolved. The presence of regular wormhole-type pores with 2-3 nm in diameter indicates a rearrangement of the aluminosilicate in the remaining part of the particles.

The studies on the different silicates allow for a better understanding of formation processes of porous silicates involving particle formation and nucleation. In addition the effect of different mineralizing agents has been evaluated. Dissolution and re-crystallization processes play a crucial role in the later stages of silicate formation. Nanoscopic zeolite particles grow into larger particles via such processes and partial dissolution of larger particles results in largely extended pores as exemplified on the hollow shell materials that could be obtained in a one pot reaction.

2.3.10. Research Area "Photocatalysis on Transition Metal containing Microporopus Silicates" (W. Schmidt)

Involved: U. Wilczok, X. Gao, H. Tüysüz

Objective

Quantum chains in microporous titanosilicate materials absorb light and create hole and electron pairs allowing photocatalytic conversion of substrate molecules on terminal sites of the quantum chains. Then investigation of photocatalytic conversions on such titanosilicates is subject of this research area.

Results: Titanium incorporation into the MFI structure results in a zeolite in which the titanium is present in tetrahedral coordination. Octahedral coordination of titanium is observed the microporous titanosilicate ETS-10 as illustrated in Fig. 4.

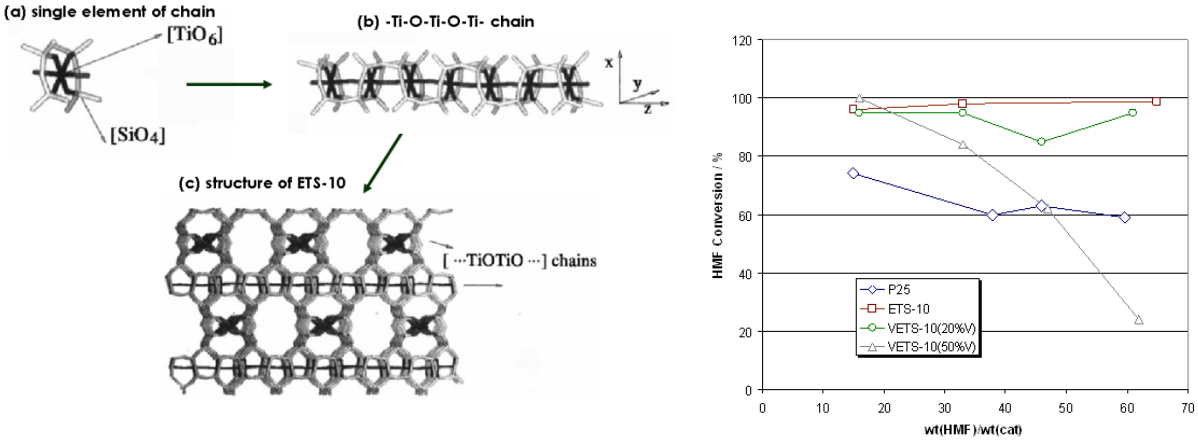

Fig. 4. ETS-10 structure (left) and photocatalytic conversion after 8h reaction time of HMF over different photocatalysts (right).

Extended titanate chains are separated by a silicate framework and thus act as quantum chains with semiconductor properties. Illumination with UV light causes charge separation and as the consequence ETS-10 is a microporous photocatalyst. In an ongoing research project the capability of ETS-10 based photocatalysts is explored. The aim is conversion of molecules that are formed in the product chain of biomass derived molecules into platform molecules for further processing. Selective oxidation of 5-hydroxymethyl furfural, a product of the conversion of sugar, to 2,5-furandicarboxylic acid is under investigation. Different ETS-10 materials have been synthesized including

materials in which titanium was replaced partially by vanadium (20% and 50% replacement of Ti by V). In comparison with the standard TiO_2 reference catalyst P25, ETS-10 based catalysts performed well and showed high conversion under UV radiation. Vanadium containing V-ETS-10 with 20% replacement of Ti by V showed conversion similar to that of the normal ETS-10 whereas V-ETS-10 with 50% replacement of Ti by V showed lower conversion at higher concentrations of HMF. Analysis of the reaction products revealed that the major reaction products were organic acids with low molecular weight. Formic acid is one of the main products whereas little conversion to carbon dioxide is observed. Thus, HMF can be efficiently converted under UV radiation but the aimed product, namely 2,5-furandicarboxylic acid, is formed only in small amounts. It seems that the primary oxidation products get fragmented and formic acid is then found as the major product.

2.3.11 Research Area "Supported Transition Metal Oxide Catalysts for Low Temperature Application" (W. Schmidt)

Involved: J. Tseng, C. Weidenthaler, A. Pommerin, C. Gawlik

Objective

Certain transition metal oxides, such as cobalt oxide, have been shown to be efficient catalysts for the conversion of CO at ambient conditions. The investigation of supported transition metal based catalysts as low temperature catalyst for alternative conversions is subject of this research area.

Results: Transition metal catalysts that are supported on activated carbons have been synthesized and tested for the conversion of NO_2 under ambient conditions. The research focuses on potential catalysts that can catalyze reactions at ambient conditions. The working principal comprises two steps, i.e. adsorption of noxious gases on an activated carbon followed by catalytic decomposition of the molecules on the catalyst

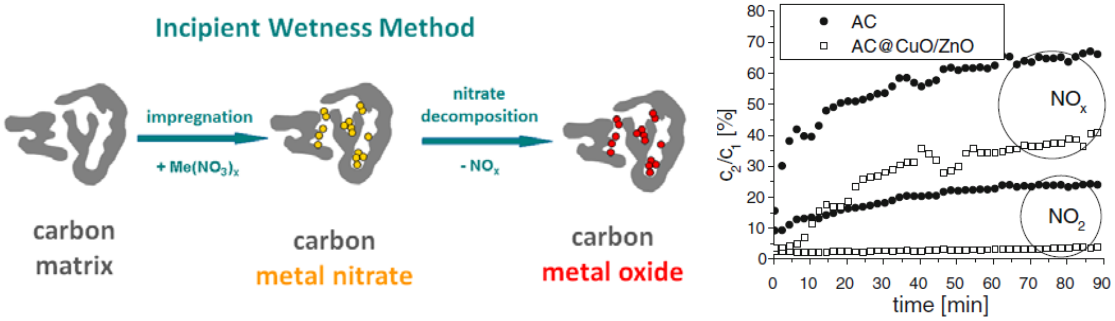

Fig. 1. Preparation of activated carbon (AC) supported transition metal catalyst via wet impregnation (left) and breakthrough curves of NO_x and NO_2 through AC@CuO/ZnO and AC after 6 cycles (right, 23 °C, 50 % r. H., c_1 NO_2 = 4 ppmV, v = 0.2 m/s). [81]

deposited within the pores of the carbon. Different methods for the deposition of pure transition metal oxides (see Fig. 1, left) as well as mixtures thereof have been investigated, i.e. liquid phase impregnation with aqueous transition metal salts or alternatively deposition of oxide precursors via chemical vapor phase deposition [76,82]. The investigations have been performed in collaboration with the Institut für Energie- und Umwelttechnik (IUTA, Duisburg) and the University of Duisburg-Essen.

Hopcalite and mixed CuO/ZnO catalysts showed best performance, especially after successive adsorption cycles as shown in Fig. 1 for CuO/ZnO on activated carbon [82]. In comparison to the pure activated carbon, the NO_x concentration could be reduced significantly. NO_2 is reduced to NO at the carbon surface, a reaction that is also

observed for pure activated carbon. However, the breakthrough curve showing NO_x as the sum of NO_2 and NO for AC@CuO/ZnO proves that the amount of total NO_x is reduced in the presence of the transition metal oxide catalysts.

Transition metal catalysts that are deposited within activated carbons via chemical vapour phase deposition have also been tested for the conversion of NO_2 at a somewhat higher temperature of 150°C. Under these conditions also iron oxide nanoparticles in activated carbon showed conversion of NO_2 to NO that was followed by decomposition of NO to N_2 and CO_2.

2.3.12 Research Area "Design of Nanostructured Materials with High Surface Area for Photo-Electrochemical Water Splitting" (H. Tüysüz)

Involved: G. Dodekatos, T. Grewe, X. Deng

Objective: In this ongoing and planned research project, a systematic and integrated approach encompassing materials synthesis, *in-situ* structural and electrochemical characterization, as well as catalytic and photocatalytic evaluation particularly for water splitting, which is one of the appealing reactions toward development of sustainable energy sources, is carried out. The main goals of this research are design and development of highly active nanocrystals and ordered mesoporous composite (binary and ternary) electro- and photo-catalysts with heterojunctions by using templating processing and post-treatment, in addition to establishment of design rules in terms of particle size, morphology, pore volume and size, surface area, crystallinity and composition for engineered ordered mesoporous photocatalyst materials, and the study of individual effects of material's properties that are responsible for the effective charge separation and catalytic activity.

Results: Even two decades after the discovery of ordered mesoporous materials (OMMs), there is still a great interest in design of OMMs and improvement of synthetic approaches. This class of material supplies many fascinating properties that make them outstanding in a range of applications, in particularly in heterogeneous catalysis as support and catalyst.[32] Some of our efforts are devoted to better understanding of the nanocasting methodology and development of novel functional high surface area materials based on transition metal oxides[4,20,28]. A significant effect has been discovered for the replication of ordered mesoporous Cr_2O_3 and iron doped Co_3O_4. In contrast to the published studies, when cubic ordered mesoporous KIT-6 with 100°C aging temperature is used as a hard template, a cubic ordered mesoporous Cr_2O_3 replica with an uncoupled sub-framework structure that possesses an additional (110) reflection and reduced symmetry is obtained. Furthermore, it is noticed that the structure, morphology and symmetry of the Co_3O_4 replica can be tuned by iron doping during the nanocasting process. A small addition of iron during the impregnation forces Co_3O_4 to develop only in one pore system of the double gyroid silica template in some regions of the parent template, resulting in a replica with lower symmetry, higher pore volume and bi-modal pore size distribution. These findings demonstrate for the first time that the growth mechanism of metal oxides in the channels of the gyroid silica is not only

related to the interconnectivity of the silica template, it also depends on the type and nature of the metal oxide precursor.

We aim to develop novel ordered mesoporous composite materials and examine them as photo and electro-catalyst for water splitting. We initialized our first electrochemical study on ordered mesoporous Co_3O_4.[85] A series of Co_3O_4 with different morphologies, symmetries, surface areas and particle sizes has been prepared by changing the textural parameters of the silica hard template via nanocasting. These materials were tested as electrocatalysts for water splitting. The highest catalytic activity was achieved in a more concentrated alkali solution with Co_3O_4 that has an open sub-framework structure and high surface area. Co_3O_4 with the highest surface area has much better activities than its bulk counterpart and slightly higher activity than material with nanoparticle morphology. The nanocast Co_3O_4 has excellent structural stability that is retained during the electrolysis of water. This material holds promise as a cheap anode for overall water splitting.[85]

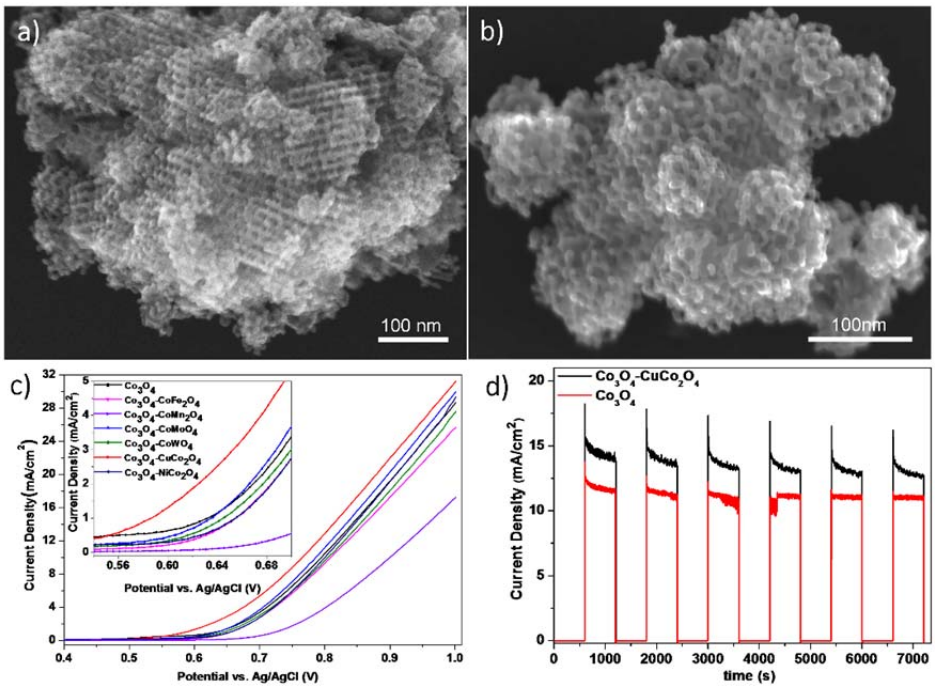

Figure 1. HR-SEM images of ordered mesoporous Co_3O_4 (a) and Co_3O_4-$CuCo_2O_4$ (b) that has been prepared via nanocasting by using silica as hard template. Oxygen evolution currents of as-made Co_3O_4, Co_3O_4-CoM_2O_4 (M= Fe, Mn), Co_3O_4-$CoMO_4$ (M = Mo, W) and Co_3O_4-MCo_2O_4 (M = Cu, Ni) composites dispersed on glassy carbon electrode in 0.1 M KOH electrolyte (c), the inset figure shows the current increment in a narrow voltage range (0.54 ~ 0.70 V vs. Ag/AgCl). Chronoamperometric measurement of Co_3O_4 and Co_3O_4-$CuCo_2O_4$ under a bias of 0.8 V vs. Ag/AgCl for 6000 sec (d) indicating stability of the materials.

Our further study was on enhancement of the electrocatalytic activates of nanocast Co_3O_4. The second generation electrocatalysts are based on binary mixed ordered mesoporous oxides. The surface of nanocast Co_3O_4 could be successfully modified by a

solid-solid reaction with various transition metal salts [24]. The novel method that we develop provides a blueprint for the production of composite materials based on ordered porous oxides that could have interesting physical and chemical properties (Figure 1a-b).[49]

The catalytic activity of the composite materials was studied in electrochemical water splitting, and the Co_3O_4-$CuCo_2O_4$ was found to be most active, with a lower onset potential and higher current density than pure Co_3O_4 (Figure 1c-d). This work opens up new possibilities in developing functional materials with ordered structure and high surface area based on non-precious metal catalysts.[46] A further study concerning the combination of this anode material with a high surface area semiconductor material for photo–electrochemical water splitting is in progress.

The design of third generation electrocatalysts will be based on ternary mixed metal oxides. A study concerning the fabrication of novel ordered mesoporous metal oxide/alloys is in progress as well. In particularly, Co_3O_4/CoPt, CuO/CuPt materials are thought to be remarkable as electrocatalyst based on the previously obtained results. Besides the synthesis and catalytic investigation, a study concerning the conductivity and charge transport on the prepared materials is planned to be carried out to understand the main reason for the catalytic enhancement. For that purpose, there will be an external collaboration with Dr. Steven J. Konezny (Yale University, USA).

Some part of our research is also focused on development of semiconductor nanostructured materials where the effects of junctions between two crystal structures for photocatalytic hydrogen production is studied. A project in collaborating with Prof. C. Chan (Arizona State University, USA) has been started on sodium tantalum oxide based materials since they are among the most stable and active photocatalysts. By a novel method, precisely controlling the reaction parameters, we could fabricate amorphous porous $NaTaO_x$, crystalline $NaTaO_3$ and crystalline $Na_2Ta_2O_6$ with morphologies that consist of a porous structure with interconnected nanoparticles or nanoparticles only. The photocatalytic investigation for overall water splitting indicated that catalytic activity highly depends on the crystal structure and morphology of the samples, with a maximum catalytic activity obtained for crystalline $Na_2Ta_2O_6$ with a nanoparticle and porous matrix structure. It seems that the junctions between two phases or morphologies of sodium tantalum oxides have an important effect on the material's catalytic behavior.[86]

Following this observation, a novel series of sodium tantalum oxide is fabricated to investigate the junctions between two different sodium tantalates.[87] It was shown that the crystal structure, band gap, morphology and textural parameters of sodium tantalates

can be controlled via a feasible hydrothermal route by changing the pH and reaction time. $Na_2Ta_2O_6$ with pyrochlore-type structure, that has an average particle size of around 27 nm, is synthesized at low alkali concentration. By slightly increasing the alkali concentration, another $Na_2Ta_2O_6$ sample with an average particle size of 15 nm and higher surface area is prepared (Figure 2a). Further increasing the alkali concentration results in a series of composite materials based on a mixture of $Na_2Ta_2O_6$ and $NaTaO_3$ (Figure 2b-c). In addition, large $NaTaO_3$ cubes are prepared at very high alkali conditions (Figure 2d). The catalytic activities of the prepared samples are investigated for photocatalytic hydrogen production and their efficiencies are correlated to the composition, surface area and junction between the two crystal structures of the materials (Figure 2e). The highest photocatalytic activity is achieved with $Na_2Ta_2O_6$ nanoparticles with the highest surface area. It is noticed that the hydrogen production rate is not only correlated to the high surface areas of the materials, an enhanced H_2 production is obtained for composite materials that is attributed to junctions between the pyrochlore and perovskite phases of sodium tantalite.[87]

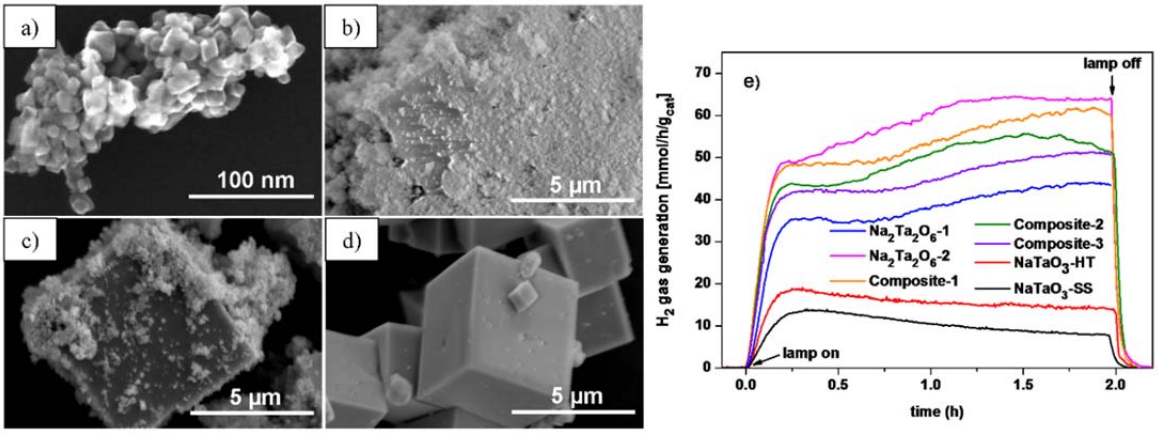

Figure 2. SEM images of $Na_2Ta_2O_6$-2 (a), Composite-2 (b), Composite-3 (c) and $NaTaO_3$-HT (d). Hydrogen production rate of the sodium tantalates prepared by hydrothermal route and the reference material $NaTaO_3$ produced via a solid-solid state.

The above investigations have proven that there is a clear effect of the junctions between two crystal phases of sodium tantalum oxide, which is mainly due to the better charge transfer and separation of electron and holes. A better junction may affect photo-catalytic activity of the material even stronger. In order to study that, systematic studies on design of nanocrystals that have two crystal phases in the same particle are in progress. In addition, a composite material in an ordered mesoporous form might provide much better catalytic activity due to the distinctive material properties like high surface area (provides higher catalytic site), tailored porosity and narrow pore size distribution (allow preparation of composite structure with high heterojunction area and incorporation of catalytically active and selective species such as co-catalysts or

plasmonic nanoparticles), controllable composition and crystallinity (provide flexible composition and crystallinity control that affect material's physical properties including light absorption efficiency and charge transfer). For this purpose, a study related to the preparation of ordered mesoporous composite tantalum oxide and sodium tantalum oxide is in progress as well.

2.3.13 Research Area "Advanced X-ray Diffraction Techniques" (C. Weidenthaler)

Involved: A. Dangwal Pandey, M. Felderhoff, U. Holle, C.J. Jia, A. Pommerin, W. Schmidt, V. Tagliazucca, J. Ternieden, J.C. Tseng, H. Tüysüz, A. Wosylus

Objective: Advanced laboratory X-ray diffraction techniques are crucial for the understanding of complex systems and for the establishment of structure-property relationships in catalysis. In-situ techniques and sophisticated data analysis methods are applied in close cooperation with the catalysis groups in order to elucidate the structural details of catalytic materials and to correlate them with the performance of the solids in the catalytic reactions. Moreover, also the limits of the methods are being extended, with a focus on laboratory techniques.

Results: As a continuation of detailed crystallographic investigations of complex aluminum hydrides (see report 2008-2010), powder diffraction studies were extended to aluminum hydrides with cations of higher atomic numbers $(EuAlH_4)_2$, $Sr(AlH_4)_2$.[19] The crystal structures of new members of the family of aluminum hydrides could be solved from heavily overlapping and less resolved XRD patterns by simulated annealing. A major focus of the studies was on the understanding of phase and structure changes during the decomposition of complex aluminum hydrides by means of in situ high temperature X-ray diffraction. The studies reveal also the appearance of new intermediate hydride structures which could be studied in detail. Knowledge about the crystal structures and their structural relationships contributes to the fundamental understanding of the crystal chemistry and the chemical properties of complex aluminum hydrides.

Many of the studies of hydrides have to be carried out in a controlled sample environment. This is even more important in heterogeneously catalyzed reactions. Such in-situ experiments are mostly performed at large facility synchrotron radiation sources providing high intensity radiation and a very flexible experimental setup. However, the experimental time at such facilities is very restricted. Over the last year, a reaction chamber has been adapted on a conventional laboratory powder diffractometer. The catalysis chamber is linked to a gas distribution station which allows the adjustment of the reaction gas flows accordingly to conventional catalysis experiments. This setup enables in situ investigations of catalysts during a catalytic reaction on laboratory instruments also over a long and flexible time period and with high quality data.

Nanostructured hematite (Fe_2O_3), encapsulated in a porous silica shell, was studied in detail with respect to structural changes during the decomposition of ammonia.[11] The sample was prepared on a sieve plate into a ceramic sample holder and heated up from room temperature to 800 °C in a dry NH_3 atmosphere. The reaction gas flowed through the sample with a flow rate set to 15000 cm^3/g h. The analysis reveals a complex sequence of crystalline iron oxide, iron nitride, and metallic iron phases. Additionally, the chemical composition and the crystal structures of the iron nitrides formed between 450 and 700°C change with temperature and time exposed to ammonia. In comparison to the in situ studies, ex situ diffraction experiments performed in parallel emphasize, that phase changes can occur after removing samples from the reaction environment.

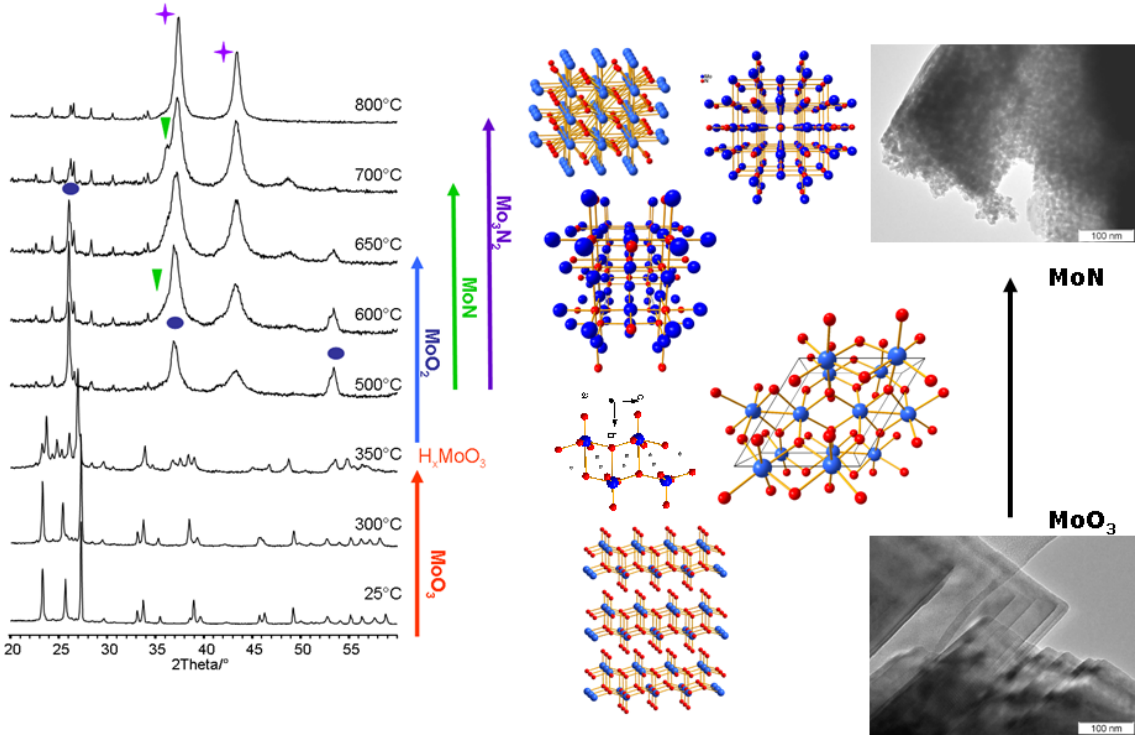

Fig. 1: In situ investigations of the formation of nanosized Mo_xN_y catalysts during the ammonolysis of large MoO_3 crystals

Another type of material investigated as potential catalysts for ammonia decomposition were nanostructured molybdenum nitrides. The entire formation pathway of the nitrides by ammonolyses of oxides was studied qualitatively and quantitatively by in situ XRD and the data were correlated with the catalytic performance (Fig. 1).[40]

These in-house experiments do not only provide a qualitative information on the crystalline catalyst phases involved, but also a quantitative analysis of the sample composition over the entire temperature range. The variation of the chemical composition of the individual phases can be analyzed in detail, and microstructure properties, such as size and defect concentrations, can be evaluated in parallel. The

comprehensive dataset of structural properties can be directly related to the catalytic properties of a distinct catalyst (Fig. 2).

However, it is not only the chemical and the phase composition which influence catalytic performance, it is widely accepted that the microstructure of solid catalysts (defined as domain size and different types of defects) also significantly influence the catalytic properties.

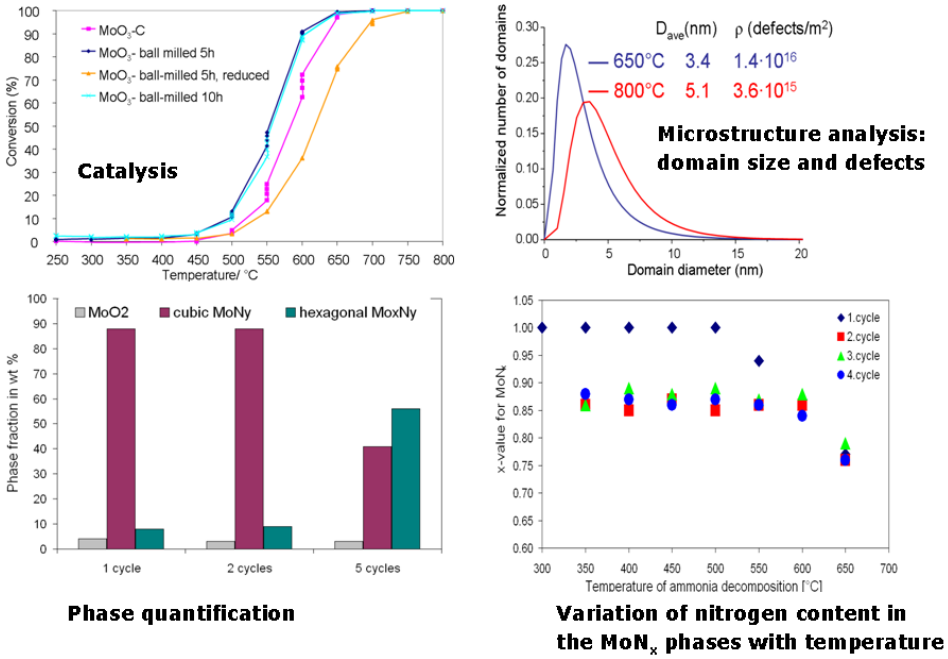

Fig. 2: Results obtained from diffraction experiments and catalytic testing.

Usually, the different types of defects are analyzed by electron microscopy techniques. However, electron microscopy images are often not representative for the entire catalyst sample. To overcome this problem, modern approaches for the evaluation of microstructure properties from powder diffraction data (line profile analyses) have been implemented in the group. The method was used to study the influence of the microstructure of Co_3O_4 on the catalytic performance for CO oxidation. It has been shown, that the addition of small amounts of silica during synthesis enables the size-control of Co_3O_4 catalysts. The domain size and the size distribution were calculated from the diffraction data.[26] The most preferable size distribution with respect to the catalytic performance was obtained for Si:Co of 0.5. Without addition of silica the mean domain size is large (40 nm) and the distribution is very broad. The activity is rather low compared to the samples with narrow size distribution and small mean domains (2-4nm) (Fig. 3). Additionally, microstructure changes taking place under non ambient conditions are more than difficult to monitor by electron microscopy methods. One big advantage of line profile analyses methods is that in addition to the atomic structures

also changes of defect concentrations and/or domain size changes under reaction conditions can be investigated.[43]

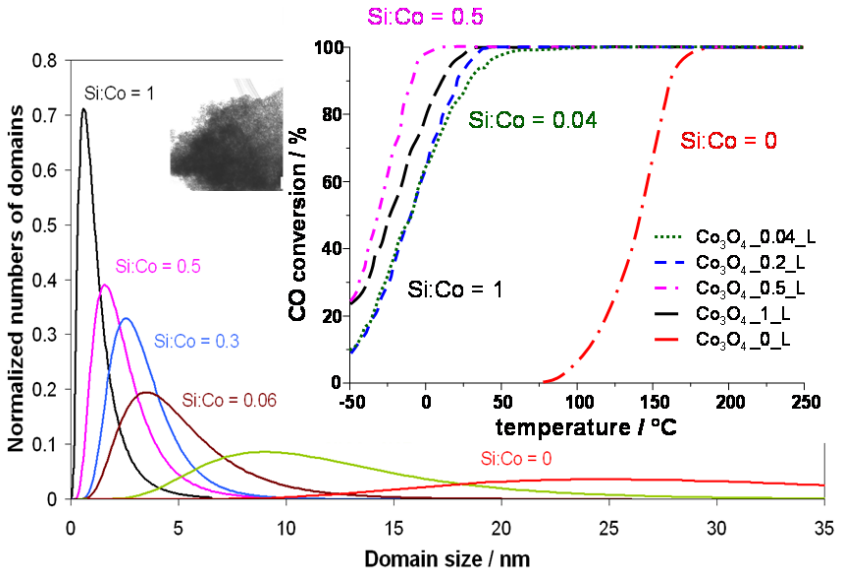

Fig. 3: Variation of size distribution in dependence of Si:Co ratio and influence on low temperature CO oxidation properties.

Microstructure changes of Cr_2O_3 due to ball milling or different temperature treatments have been intensively studied by diffraction methods. In situ studies of mesostructured Cr_2O_3 with interesting magnetic properties performed at lower temperatures (between 220 and 360 K) trace structural changes depending on the synthesis temperatures.[28] In addition to differences on the atomic level, also temperature dependent changes of the crystallite shape are detected (Fig.4).

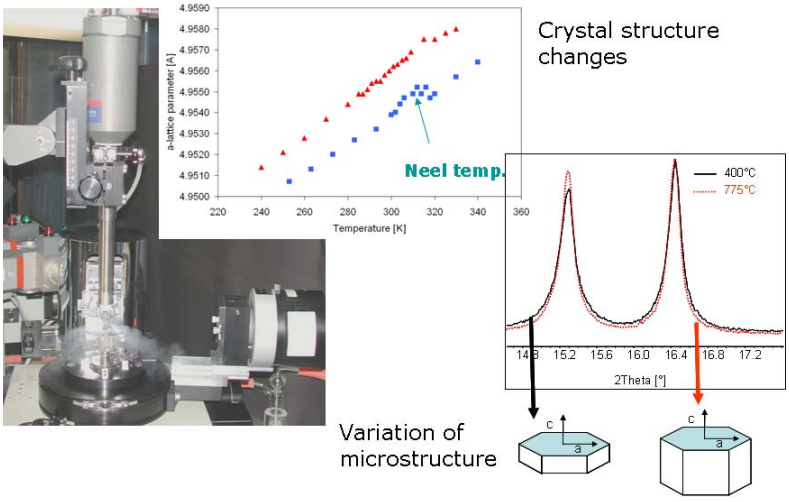

Fig. 4: Diffraction experiments performed in-house at low temperatures, dependence of microstructure properties (morphology changes) on the change of the synthesis temperatures.

2.3.14 Publications 2011-2013 from the Department of Heterogeneous Catalysis

The publications are listed separately for each group of the Department. Many of the publications result from more than one group and therefore appear more than once. In order to avoid the impression that more publications are listed than have actually appeared, such publications are assigned identical numbers. As a consequence the numbering does not appear strictly ascending in this list.

Schüth Group

(1) Onfroy, T.; Li, W.-C.; Schüth, F.; Knözinger, H. *Top. Catal.* **2011**, *54*, 390-397

(2) Schüth, F. *Chem. Ing. Tech.* **2011**, *83*, 1984-1993

(3) Jia, C.J.; Schüth, F. *Phys. Chem. Chem. Phys.* **2011**, *13*, 2457-2487

(4) Benitez, M.; Petracic, O.; Tüysüz, H.; Schüth, F.; Zabel, H. *Phys. Rev. B* **2011**, *83*, 134424-134424

(5) Güttel, R.; Paul, M.; Schüth, F. *Catal. Sci. Technol.* **2011**, *1*, 65-68

(6) Shao, H.; Felderhoff, M.; Schüth, F.; Weidenthaler, C. *Nanotechnol.* **2011**, *22*, 235401/1-235401/7

(7) Wang, G.H.; Li, W.C.; Jia, K.-M.; Lu, A.H.; Feyen, M.; Spliethoff, B.; Schüth, F. *NANO* **2011**, *6*, 469-479

(8) Asahina, S.; Uno, S.; Suga, M.; Stevens, S.M.; Klingstedt, M.; Okano, Y.; Kudo, M.; Schüth, F.; Anderson, M.; Adschiri, T. *Microporous Mesoporous Mater.* **2011**, *146*, 11-17

(9) Schüth, F. *Prax. Naturwiss., Chem. Sch.* **2011**, *60*, 8-13

(10) Schüth, F. *Phys. Chem. Chem. Phys.* **2011**, *13*, 2447-2448

(11) Feyen, M.; Weidenthaler, C;, Guettel, R.; Schlichte, K.; Holle, U.; Lu, A.H.; Schüth, F. *Chem.-- Eur. J.* **2011**, *17*, 598-605

(12) Galeano, C.; Guettel, R.; Michael, P.; Arnal, P.; Lu, A.H.; Schüth, F. *Chem.-- Eur. J.* **2011**, *17*, 8434-8439

(13) Bathen, D.; Burfeind, J.; Felderhoff, M.; Hausschild, K.; Hesske, C.; Peil, S.; Schüth, F.; Urbanczyk, R. *Fuel Cells* **2011**, *11*, 911-920

(14) Bongard, H.J.; Hao, G.P.; Li, W.C., Lu A.H.; Qian, D.; Schüth, F; Wang, A.Q.; Wang, G.H.; Zhang, W.P.; Zhang, T *J. Am. Chem. Soc.* **2011**, *133*, 11378-11388

(15) Jia, C.J.; Schwickardi, M.; Weidenthaler, C.; Schmidt, W.; Korhonen, S.; Weckhuysen, B.; Schüth, F. *J. Am. Chem. Soc.* **2011**, *133*, 11279-11288

(16) Shao, H.; Felderhoff, M.; Schüth F. *Int. J. Hydrogen Energy*, **2011**, *36*, 10828–10833

(17) Schüth, F. *Chem. Mater.* **2012**, *24*, 1-2
(18) Kaper, H.; Grandjean, A.; Weidenthaler, C.; Schüth, F.; Goettmann, F. *Chem.--Eur. J.* **2012**, *18*, 4099-4106
(19) Pommerin, A.; Wosylus, A.; Felderhoff, M.; Schüth, F.; Weidenthaler, C. *Inorg. Chem.* **2012**, *51*, 4143-4150
(20) Tüysüz, H.; Weidenthaler, C.; Schüth, F. *Chem.--Eur. J.* **2012**, *18*, 5080-5086
(21) Schüth, F.; Palkovits, R.; Schloegl, R.; Su, D.S. *Energy & Environ. Sci.* **2012**, *5*, 6278-6289
(22) Meier, J.C.; Galeano, C.; Katsounaros, I.; Topalov, A.A.; Kostka, A.; Schüth, F.; Mayrhofer, K.J.J. *ACS Catal.* **2012**, *2*, 832-843
(23) Meine, N.; Rinaldi, R.; Schüth, F. *ChemSusChem* **2012**, *8*, 1449 - 1454
(24) Tüysüz, H.; Salabas, E.; Bill, E.; Bongard, H.; Spliethoff, B.; Lehmann, C.W.; Schüth, F. *Chem. Mater.* **2012**, *24*, 2493-2500
(25) Guettel, R.; Paul, M.; Galeano, C.; Schüth, F. *J. Catal.* **2012**, *289*, 100-104
(26) Dangwal- Pandey, A.; Jia, C.; Schmidt, W.; Matteo, L.; Schwickardi, M.; Schüth, F.; Weidenthaler, C. *J. Phys. Chem. C* **2012**, 116, 19405-19412
(27) Meier, J.C.; Katsounaros, I.; Galeano, C.; Bongard, H.; Topalov, A.A.; Kostka, A.; Karschin, A.; Schüth, F.; Mayrhofer, K.J.J. *Energy Environ. Sci.* **2012**, *5*, 9319-9330
(28) Tüysüz, H.; Weidenthaler, C.; Grewe, T.; Salabas, E.; Benitez-Romero, M.; Schüth, F. *Inorg. Chem.* **2012**, *51*, 11745-11752
(29) Galeano, C.; Meier, J.C;, Peinecke, V.; Bongard, H.; Katsounaros, I.; Topalov, A.A;, Lu, A.H.; Mayrhofer, K.J.J.; Schüth, F. *J. Am Chem. Soc.* **2012**, *134*, 20.457-20.465
(30) Jiang, H.; Bongard, H.; Schmidt, W.; Schüth, F. *Microporous Mesoporous Mater.* **2012**, *164*, 3-8
(31) Schubert, U.; Nestle, I.; Engel, K.; Schüth, F. *Nachr. Chem.* **2012**, **60**, 784 - 785
(32) Tüysüz, H.; Schüth, F. *Adv. Catal.* **2012**, *55*, 127-239
(33) Schüth, F. *Chemical Energy Storage*; Schlögl, R., Ed., De Gruyter, Berlin/Boston, **2013**, pp 35-48
(34) Hilgert, J.; Meine, N.; Rinaldi, R.; Schüth, F. *Energy Environ. Sci.* **2013***, 6*, 92-96
(35) Zheng, W.; Cotter, T.P.; Kaghazchi, P.; Jacob, T.; Frank, B.; Schlichte, K.; Zhang, W.; Su, D.S.; Schüth, F.; Schlögl, R. *J. Am. Chem. Soc.* **2013**, *135*, 3458-3464
(36) Richter, F.; Pupovac, K.; Palkovits, R.; Schüth, F. *ACS Catal.* **2013**, *3*, 123-127

(37) Soorholtz, M.; White, R.J.; Zimmermann, T.; Titirici, M.M.; Antonietti, M.; Palkovits, R.; Schüth, F. *Chem. Commun.* **2013**, *49*, 240-242
(38) Schüth, F. *Phys. Sataus Solidi B* **2013**, *250*, 1142-1151
(39) Lim, I.H.; Schrader, W.; Schueth, W. Microporous Mesoporous Mater. **2013**, *166*, 20-36
(40) Tagliazzucca, V.; Schlichte, K.; Schüth, F.; Weidenthaler, C. *J. Catal.* **2013**, *305*, 277 – 289
(41) Carrasquillo-Flores, R.; Kaldstrom, M.; Dumesic, J.A.; Rinaldi, R.; Schüth, F. *ACS Catal.* **2013**, *3*, 993 – 997
(42) Schmidt, W.; Schüth, F.; Weidenthaler, C. *Comprehensive Inorganic Chemistry II*, Poeppelmeier, K.; Reedijk, J., Eds.; Elsevier, **2013**; pp 1-24
(43) Immohr,S.; Felderhoff,M.; Weidenthaler,C.; Schüth, F. *Angew. Chem., Int. Ed.* **2013**, *52*, 12688–1269
(44) Galeano, C.; Baldizzone, C.; Bongard, H.; Spliethoff, B.; Weidenthaler, C.; Meier, J.C.; Mayrhofer, K.J.J.; Schüth, F. *Adv. Funct. Mater.* **2013**, *24*, 220–232.
(45) Gu, D.; Schüth, F. *Chem. Soc. Rev.* **2013**, *43*, 313-44
(46) Richter, F.; Meng, Y.; Klasen, T.; Sahraoui, L.; Schüth, F. *J. Catal* **2013**, *308*, 341-351
(47) Wang, G.H. ; Hilgert, J.; Richter, F.; Wang, F.; Bongard, H-J; Spliethoff, B.; Weidenthaler, C.; Schüth, F. *Nat. Mat.* **2013**, accepted
(48) Trotus, T.; Zimmermann, T.; Schüth., F. *Chem. Rev.* **2013**, DOI: 10.1021/cr400357r
(49) Grewe, T.; Deng X.; Weidenthaler, C.; Schüth, F., Tüysüz, H. *Chem. Mat.* **2013**, *25*, 4926–4935

Schüth Group / Felderhoff

(6) Shao, H.; Felderhoff, M.; Schüth, F.; Weidenthaler, C. *Nanotechnol.* **2011**, *22*, 235401/1-235401/7
(13) Bathen, D.; Burfeind, J.; Felderhoff, M.; Hauschild, K.; Hesske, C.; Peil, S.; Schüth, F.; Urbanczyk, R. *Fuel Cells* **2011**, *11*, 911-920
(16) Shao, H.; Felderhoff, M.; Schüth F. *Int. J. Hydrogen Energy*, **2011**, *36*, 10828–10833
(19) Pommerin, A.; Wosylus, A.; Felderhoff, M.; Schüth, F.; Weidenthaler, C. *Inorg. Chem. **2012**, 51, 4143-4150*
(43) Immohr,S.; Felderhoff,M.; Weidenthaler,C.; Schüth, F. *Angew. Chem., Int. Ed.* **2013**, DOI: 10.1002/ange.201305992

(50) Felderhoff, M.; Zibrowius, B. *Phys. Chem. Chem. Phys.* **2011**, *13*, 17234–17241
(51) Weidenthaler, C.; Felderhoff M. *Energy Environ. Sci.* **2011**, *4*, 2495–2502.
(52) Felderhoff, M.; Urbanczyk, R.; Peil, S. *H_2 – Das Magazin für Wasserstoff und Brennstoffzellen* **2011**
(53) Urbanczyk, R.; Peinecke, K.; Felderhoff, M.; Hauschild, K.; Peil, S. *Wasserstofftechnik*; Lehmann, J., Luschtinetz, T., Eds.; Fachhochschul.: Stralsund, **2012,** 111 - 115
(54) Felderhoff, M.; Urbanczyk, R.; Peil, S. *Green* **2013**, *3*, 113–123

Marlow group

(55) Khan, T. R.; Erbe, A.; Auinger, M.; Marlow, F.; Rohwerder, M. *Sci. Technol. Adv. Mater.* **2011**, *12*, 1-9
(56) Muldarisnur, M.; Marlow, F. *J. Phys. Chem. C* **2011**, *115*, 414–418
(57) Marlow, F.; Muldarisnur M.; Sharifi, P.; Zabel, H. *Phys. Rev. B* **2011**, *84*, 073401-073404
(58) Khan, T., Vimalanandan, A.; Marlow, F.; Erbe, A.; Rohwerder, M. *ACS Appl. Mater. Interfaces* **2012**, *4*, 6221-6227
(59) Muldarisnur, M.; Popa, I.; Marlow, F. *Phys. Rev. B* **2012**, *86,* 024105
(60) Sharifi, P.; Eckerlebe, H.; Marlow, F. *Phys. Chem. Chem. Phys.* **2012**, *14*, 10324–10331
(61) Schunk, D.; Hardt, S.; Wiggers, H.; Marlow, F. *Phys. Chem. Chem. Phys.* **2012**, *14,* 7490 – 7496
(62) Deng, T.S.; Marlow, F. *Chem. Mater.* **2012**, *24*, 536-546.
(63) Schunk, D.; Marlow, F. *NanoEnergie* **2012**, *7* (CENIDE Newsletter Juni 2012)
(64) Wiggers, H.; Schunk, D.; Marlow, F. *Unikate Universität Duisburg-Essen* **2013,** *43,* 42-51
(65) Deng, T.S.; Sharifi, P.; Marlow, F. *ChemPhysChem* **2013**, *14*, 2893-2896
(66) Khan, T.R.; Vimalanandan, A.; Erbe, A.; Marlow, F.; Rohwerder, M. *Z. Phys.Chem.* **2013**, *227*, 1083-1095

Rinaldi group

(23) Meine, N.; Rinaldi, R.; Schüth, F. *ChemSusChem* **2012**, *5*, 1449-1454
(34) Hilgert, J.; Meine, N.; Rinaldi, R.; Schüth, F. *Energy Environ. Sci.* **2013**, *6*, 92-96

(41) Carrasquillo-Flores, R.; Käldström, M.; Schüth, F.; Dumesic, J.; Rinaldi, R. *ACS Catal.* **2013**, *3*, 993−997

(67) Rinaldi, R. *Chem. Comm.* **2011**, *47*, 511-513

(68) Jäger, G.; Girfoglio, M.; Dollo, F.; Rinaldi, R.; Bongard, H.; Commandeur, U.; Fischer, R.; Spiess, A. C.; Büchs, J. *Biotechnol. Biofuels* **2011**, *4*, 33

(69) Engel, P.; Bonhage, B.; Pernik, D.; Rinaldi, R.; Schmidt, P.; Wulfhorst, H.; Spiess, A.C. *Comput-Aided Chem. Eng.* **2011**, *29*, 1316-1320

(70) Wang, X.; Rinaldi, R. *Energy Environ Sci* **2012**, *5*, 8244-8260

(71) Wang, X.; Rinaldi, R. *ChemSusChem* **2012**, *5*, 1455-1466

(72) Rinaldi, R. *J. Chem. Eng. Data* **2012**, *57*, 1341-1343

(73) Wang, X.; Rinaldi, R. *Angew. Chem., Int. Ed.* **2013**, *52*, 11499-11503

(74) Loerbroks, C.; Rinaldi, R.; Thiel, W. *Chem.--Eur. J.* **2013**, *19,* 16282-16294

(75) Rinaldi, R.; Reece, J. Catalysis for the Conversion of Biomass and Its Derivatives. In *Max Planck Research Library for the History and Development of Knowledge, Proceedings 2,* Behrens, M.; Abhaya D., Eds.;. Berlin **2013**

Schmidt group

(15) Jia, C.J.; Schwickardi, M.; Weidenthaler, C.; Schmidt, W.; Korhonen, S.; Weckhuysen, B.; Schüth, F. *J. Am. Chem. Soc.* **2011**, *133*, 11279-11288

(26) Dangwal- Pandey, A.; Jia, C.; Schmidt, W.; Matteo, L.; Schwickardi, M.; Schüth, F.; Weidenthaler, C. *J. Phys. Chem. C* **2012**, *116*, 19405-19412

(30) Bongard, H.; Jiang, H.; Schmidt, W.; Schüth, F. *Microporous Mesoporous Mater.* **2012**, *164*, 3-8

(42) Schmidt, W.; Schüth, F.; Weidenthaler, C. *Comprehensive Inorganic Chemistry II*, Poeppelmeier, K.; Reedijk, J., Eds.; Elsevier, 2013; pp 1-24

(76) Busch M.; Bergmann, U.; Sager, U.; Schmidt, W.; Schmidt, F.; Notthoff, C.; Atakan, B.; Winterer, M. *J. Nanosci. Nanotechnol.* **2011**, *11*, 7956 – 7961

(77) Gu, X.; Zhu, W.; Jia, C.R.; Zhao, R.; Schmidt, W.; Wang, Y. *Chem. Commun.* **2011**, *47*, 5337 – 5339

(78) Gu, X.; Jiang, T.; Tao, H.; Zhou, S.; Liu, X.; Ren, J.; Wang, Y.; Lu, G.; Schmidt, W.
J. Mater. Chem. **2011**, *21*, 880 – 886

(79) Gu, X.; Tao, H.; Schmidt, W.; Lu, G.; Wang, Y. *J. Mater. Chem.* **2012**, *22*, 2473 – 2477

(80) Schmidt, W. in *Ion-exchange Technology: Theory, Materials and Applications* eds. Inamuddin, I.; Luqman, M., Eds.; Springer; **2012**, pp 277–298

(81) Reichinger, M.; Schmidt, W.; Narkhede, V.V.; Zhang, W.; Gies, H.; Grünert, W. *Microporous Mesoporous Mater.* **2012**, *164*, 21–31

(82) Sager, U.; Schmidt, W.; Schmidt, F.; Suhartiningsih *Adsorption* **2013***, 19*, 1027–1033

(83) Castro, M.; Haouas, M.; Taulelle, F.; Lim, I.; Breynaert, E.; Brabants, G.; Kirschhock, C.E.A.; Schmidt, W. *Micropor. Mesopor. Mater.*, **2013**, online available 03 Sep 2013

Tüysüz group

(4) Benitez, M.; Petracic, O.; Tüysüz, H.; Schüth, F.; Zabel, H. *Phys. Rev. B* **2011**, *83*, 134424-134424

(20) Tüysüz, H.; Weidenthaler, C.; Schüth, F. *Chem.--Eur. J.* **2012**, *18*, 5080-5086

(24) Tüysüz, H.; Salabas, E.; Bill, E.; Bongard, H.; Spliethoff, B.; Lehmann, C.W.; Schüth, F. *Chem. Mater.* **2012**, *24*, 2493-2500

(28) Tüysüz, H.; Weidenthaler, C.; Grewe, T.; Salabas, E.; Benitez-Romero, M.; Schüth, F. *Inorg. Chem.* **2012**, *51*, 11745-11752

(32) Tüysüz, H.; Schüth, F. *Adv. Catal.* **2012***, 55*, 127-239

(49) Grewe, T.; Deng X.; Weidenthaler, C.; Schüth, F., Tüysüz, H. *Chem. Mat.* **2013**, DOI: 10.1021/cm403153u

(84) Deng, Y.; Tüysüz, H.; Henzie, J.; Yang, P. *Small,* **2011**, *7*, 2037-2040

(85) Tüysüz, H,: Hwang, Y.; Khan, S. B.; Asiri, A. M.; Yang, P. *Nano Res.* **2013**, *6*, 47-54

(86) Tüysüz, H.; Chen, C. *Nano Energy* **2013**, *2*, 116-123

(87) Grewe, T.; Meier, K.; Tüysüz, H. *Catal. Today* **2013**, DOI:10.1016/j.cattod.2013.10.092

Weidenthaler group

(6) Shao, H.; Felderhoff, M.; Schüth, F.; Weidenthaler, C. *Nanotechnol.* **2011**, *22*, 235401/1-235401/7

(11) Feyen, M.; Weidenthaler, C;, Guettel, R.; Schlichte, K.; Holle, U.; Lu, A.H.; Schüth, F.: *Chem.-- Eur. J.* **2011**, *17*, 598-605

(15) Jia, C.J.; Schwickardi, M.; Weidenthaler, C.; Schmidt, W.; Korhonen, S.; Weckhuysen, B.; Schüth, F.: *J. Am. Chem. Soc.* **2011**, *133*, 11279-11288

(18) Kaper, H.; Grandjean, A.; Weidenthaler, C.; Schüth, F.; Goettmann, F. *Chem.--Eur. J.* **2012**, *18*, 4099-4106

(19) Pommerin, A.; Wosylus, A.; Felderhoff, M.; Schüth, F.; Weidenthaler, C. *Inorg. Chem.* **2012**, *51*, 4143-4150

(20) Tüysüz, H.; Weidenthaler, C.; Schüth, F. *Chem.--Eur. J.* **2012**, *18*, 5080-5086

(26) Dangwal- Pandey, A.; Jia, C.; Schmidt, W.; Matteo, L.; Schwickardi, M.; Schüth, F.; Weidenthaler, C. *J. Phys. Chem. C* **2012**, *116*, 19405-19412

(28) Tüysüz, H.; Weidenthaler, C.; Grewe, T.; Salabas, E.; Benitez-Romero, M.; Schüth, F. *Inorg. Chem.* **2012**, *51*, 11745-11752

(40) Tagliazucca, V.; Schlichte, K.; Schüth, F.; Weidenthaler, C. *J. Catal.* 2013, *305*, 277-289

(42) Schmidt, W.; Schüth, F.; Weidenthaler, C. Diffraction and Spectroscopy of Porous Solids In: *Comprehensive Inorganic Chemistry II*, Poeppelmeier, K.; Reedijk, J., Eds.; Elsevier, 2013; pp 1-24

(43) Immohr, S.; Felderhoff, M.; Weidenthaler, C.; Schüth, F. *Angew. Chem., Int. Ed.* **2013**, DOI: 10.1002/ange.201305992

(44) Galeano, C.; Baldizzone, C.; Bongard, H.; Spliethoff, B.; Weidenthaler, C.; Meier, J.C.; Mayrhofer, K.J.J.; Schüth, F. *Adv. Funct. Mater.* **2013**, DOI: 10.1002/adfm.201302239

(49) Grewe, T.; Deng X.; Weidenthaler, C.; Schüth, F., Tüysüz, H. Chem. Mat. 2013, DOI: 10.1021/cm403153u

(51) Weidenthaler C.; Felderhoff M. *Energy Environ. Sci.* **2011**, *4*, 2495-2502

(88) Weidenthaler, C *Nanoscale* **2011**, *3*, 792 – 810

(89) Gesing, T.M.; Schowalter, M.; Weidenthaler, C.; Murshed, M.M.; Nénert, G.; Mendive, C.B.; Curti, M.; Rosenauer, A.; Buhl, J.C.; Schneider, H.; Fischer, R.X.F.
J. Mater.Chem. **2012**, *22*, 18814-18823.

(90) Antic, B.; Kremenovic, A.; Jovic, N.; Pavlovic, M.B.; Jovalekic, C.; Nikolic, A.S.; Goya. G.F.; Weidenthaler, C. *J. Appl. Phys.* **2012**, *111*, 074309

Others

(91) Czuprat, O.; Jiang, H.Q. *Chem. Ing. Tech.* **2011**, *83*, 2219 – 2228

(92) Liang, F.Y.; Jiang, H.Q.; Luo, H.X.; Caro, J.; Feldhoff, A. *Chem. Mat.* **2011**, *23*, 4765 – 4772

(93) Rose, M (Rose, Marcus)[1] ; Palkovits, R *Macromol. Rapid Commun.* **2011**, *32*, 1299 – 1311

(94) Neudeck, C.; Kim, Y.Y.; Ogasawara, W.; Shida, Y.; Meldrum, F.; Walsh, D. *SMALL* **2011**, *7*, 869 – 873

(95) Palkovits, R. *Chem. Ing. Tech* **2011**, *83*, 411 – 419

(96) Palkovits, R.; Tajvidi, K.; Ruppert, A.M.; Procelewska, J. *Chem. Comm.* **2011**, *47*, 576 – 578

(97) Van de Vyver, S. ; Helsen, S. ; Geboers, J. ; Yu, F. ; Thomas, J. ; Smet, M.; Dehaen, W.; Roman-Leshkov, Y.; Hermans, I. ; Sels, B.F. *ACS Catal* **2012**, *2*, 2700 – 2704

(98) Sun, L.M. ; Zhao, X.; Jia, C.J.; Zhou, Y.X.; Cheng, X.F.; Li, P.; Liu, L.; Fan, W.L. *J. Mat. Chem.* **2012**, *22*, 23428 – 23438

(99) Cao, Z.W.; Jiang, H.Q.; Luo, H.X.; Baumann, S.; Meulenberg, W.A.; Voss, H.; Caro, J. *Catal. Today* **2012**, *193*, 2 - 7

(100) Liang, F.Y.; Jiang, H.Q.; Luo, H.X.; Kriegel, R.; Caro, J. *Catal. Today* **2012**, *193*, 95 – 100

(101) Li, P.; Zhao, X.; Jia, C.J.; Sun, H.G.; Li, Y.L.; Sun, L.M.; Cheng, X.F.; Liu, L.; Fan, W.L. *Cryst. Growth Des.***2012**, *12*, 5042 – 5050

(102) Mezzavilla, S.; Zanella, C.; Aravind, P.R.; Della Volpe, C.; Soraru, G.D. *J. Mat. Sci.* **2012**, *47*, 7175 – 7180

(103) Luo, H.X.; Jiang, H.Q.; Klande, T.; Cao, Z.W.; Liang, F.Y.; Wang, H.H. ; Caro, J. *Chem. Mat.* **2012**, *24*, 2148 – 2154

(104) Tajvidi, K.; Pupovac, K.; Kukrek, M.; Palkovits, R. *ChemSusChem* **2012**, *5*, 2139 – 2142

(105) Ruppert, A.M.; Weinberg, K.; Palkovits, R. *Angew. Chem., Int. Ed.* **2012**, *51*, 2564 – 2601

(106) Rose, M.; Palkovits, R. *ChemSusChem* **2012**, *5*, 167 – 176

(107) Sun, Q. ; Guo, CZ . ; Wang, G.H.; Li, W.C. ; Bongard, H.J. ; Lu, A.H. *Chem.--Eur. J.* **2013**, *19*, 6217 – 6220

(108) Luo, F.; Jia, C.J.; Liu, R.; Sun, L.D. ; Yan, C.H. *Mater. Res. Bull.* **2013**, *48*, 1122 – 1127

(109) Schulte, J.P.; Grass, S.; Treuel, L. *J. Raman Spectrosc.* **2013**, *44*, 247 – 254

(110) Li, P.; Zhao, X.; Jia, C.J.; Sun, H.G.; Sun, L.M.; Cheng, X.F. ; Liu, L.; Fan, W.L. *J. Mat. Chem.* **2013**, *1*, 3421 – 3429

(111) Liang, F.Y.; Partovi, K.; Jiang, H.Q.; Luo, H.X.; Caro, J. *J. Mat. Chem.* **2013**, *1*, 746 – 751

(112) Op de Beeck, B.; Geboers, J.; Van de Vyver, S.; Van Lishout, J.; Snelders, J.; Huijgen, W.J.J.; Courtin, C.M.; Jacobs, P.A.; Sels, B.F. *ChemSusChem* **2013**, *6*, 199 – 208